Figure 5

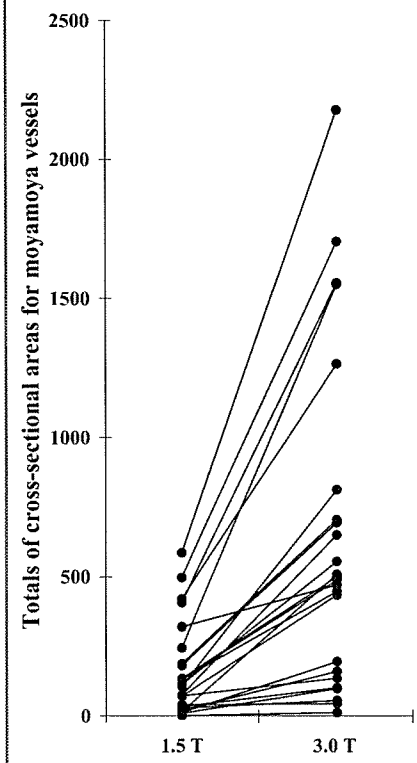

Figure 5: Graph shows the cross-sectional area of moyamoya vessels. The total cross-sectional areas for moyamoya vessels at the same level of MR angiography source images were calculated semiautomatically and compared between 3.0- and 1.5-T MR systems. Larger cross-sectional areas were visualized with 3.0-T imaging than with 1.5-T imaging. The total cross-sectional area is given as pixels.

our study demonstrated the advantages of 3.0-T imaging over 1.5-T imaging for follow-up evaluation. Although 3.0-T imaging may indeed prove advantageous in the diagnosis of moyamoya disease, larger numbers of preoperative patients should be studied in the future. In preoperative treatment planning, conventional angiography would be required because it can provide more detailed information about moyamoya vessels and other major vessels than does 3.0-T MR angiography; thus, comparative studies between 3.0-T MR angiography and conventional angiography may be needed in the future. We did not evaluate stenosis or dilatation of ICAs, anterior cerebral arteries, and MCAs because most patients had undergone conventional angiography several years before the MR examinations, which made it difficult for us to verify the findings with use of a reference standard. This is another limitation. In our study, visualization of STA-MCA bypass was not evaluated because aliasing artifacts affected STA-MCA bypass in some patients, STA-MCA bypass sites were not included in the fields of view in all patients, and most patients had undergone postoperative angiography several years before the MR examinations. Further studies may be needed to evaluate the findings of MR angiography in cases of STA-MCA bypass. Although the readers were blinded to the field strength of MR angiographic images, there were some differences in image quality of moyamoya vessels between 3.0- and 1.5-T images. It is possible that the readers were influenced by these differences.

In conclusion, moyamoya vessels are better depicted at 3.0-T 3D TOF MR angiography than at 1.5-T 3D TOF MR angiography. Radiologists must be aware of the differences, especially when patients undergo follow-up MR angiography with both 3.0- and 1.5-T MR systems.

References

1. Suzuki J, Takaku A. Cerebrovascular "moyamoya" disease: disease showing abnormal net-like vessels in base of brain. Arch Neurol 1969;20:288–299.
2. Suzuki J, Kodama N. Moyamoya disease: a review. Stroke 1983;14:104–109.
3. Fukui M. Current state of study on moyamoya disease in Japan. Surg Neurol 1997;47:138–143.
4. Chiu D, Shedden P, Bratina P, Grotta JC. Clinical features of moyamoya disease in the United States. Stroke 1998;29:1347–1351.
5. Graham JF, Matoba A. A survey of moyamoya disease in Hawaii. Clin Neurol Neurosurg 1997;99(suppl 2):S31–S35.
6. Fukui M. Guidelines for the diagnosis and treatment of spontaneous occlusion of the circle of Willis ('moyamoya' disease). Research Committee on Spontaneous Occlusion of the Circle of Willis (Moyamoya Disease) of the Ministry of Health and Welfare, Japan. Clin Neurol Neurosurg 1997;99(suppl 2):S238–S240.
7. Fujisawa I, Asato R, Nishimura K, et al. Moyamoya disease: MR imaging. Radiology 1987;164:103–105.
8. Yoon HK, Shin HJ, Lee M, Byun HS, Na DG, Han BK. MR angiography of moyamoya disease before and after encephaloduroarteriosynangiosis. AJR Am J Roentgenol 2000;174:195–200.
9. Bernstein MA, Huston J III, Lin C, Gibbs GF, Felmlee JP. High-resolution intracranial and cervical MRA at 3.0T: technical considerations and initial experience. Magn Reson Med 2001;46:955–962.
10. Edelstein WA, Glover GH, Hardy CJ, Redington RW. The intrinsic signal-to-noise ratio in NMR imaging. Magn Reson Med 1986;3:604–618.
11. Campeau NG, Huston J III, Bernstein MA, Lin C, Gibbs GF. Magnetic resonance angiography at 3.0 Tesla: initial clinical experience. Top Magn Reson Imaging 2001;12:183–204.
12. Al-Kwifi O, Emery DJ, Wilman AH. Vessel contrast at three Tesla in time-of-flight magnetic resonance angiography of the intracranial and carotid arteries. Magn Reson Imaging 2002;20:181–187.
13. Thomas SD, Al-Kwifi O, Emery DJ, Wilman AH. Application of magnetization transfer at 3.0 T in three-dimensional time-of-flight magnetic resonance angiography of the intracranial arteries. J Magn Reson Imaging 2002;15:479–483.
14. Willinek WA, Born M, Simon B, et al. Time-of-flight MR angiography: comparison of 3.0-T imaging and 1.5-T imaging—initial experience. Radiology 2003;229:913–920.
15. Gering E, Atkinson CT. A rapid method for counting nucleated erythrocytes on stained blood smears by digital image analysis. J Parasitol 2004;90:879–881.
16. Rajwa B, McNally HA, Varadharajan P, Sturgis J, Robinson JP. AFM/CLSM data visualization and comparison using an open-source toolkit. Microsc Res Tech 2004;64:176–184.
17. Morioka M, Hamada J, Todaka T, Yano S, Kai Y, Ushio Y. High-risk age for rebleeding in patients with hemorrhagic moyamoya disease: long-term follow-up study. Neurosurgery 2003;52:1049–1054.
18. Kobayashi E, Saeki N, Oishi H, Hirai S, Yamaura A. Long-term natural history of hemorrhagic moyamoya disease in 42 patients. J Neurosurg 2000;93:976–980.
19. Okada Y, Shima T, Nishida M, Yamane K, Yamada T, Yamanaka C. Effectiveness of superficial temporal artery–middle cerebral artery anastomosis in adult moyamoya disease: cerebral hemodynamics and clinical course in ischemic and hemorrhagic varieties. Stroke 1998;29:625–630.
20. Kikuta K, Takagi Y, Nozaki K, et al. Asymptomatic microbleeds in moyamoya disease: T2*-weighted gradient-echo magnetic resonance imaging study. J Neurosurg 2005;102:470–475.
21. Yamashita M, Oka K, Tanaka K. Histopathology of the brain vascular network in moyamoya disease. Stroke 1983;14:50–58.
22. Morioka M, Hamada J, Kawano T, et al. Angiographic dilatation and branch extension of the anterior choroidal and posterior communicating arteries are predictors of hemorrhage in adult moyamoya patients. Stroke 2003;34:90–95.
23. Kagawa R, Okada Y, Moritake K, Takamura M. Magnetic resonance angiography demonstrating adult moyamoya disease progressing from unilateral to bilateral involvement: case report. Neurol Med Chir (Tokyo) 2004;44:183–186.
24. Kim SK, Seol HJ, Cho BK, Hwang YS, Lee DS, Wang KC. Moyamoya disease among young patients: its aggressive clinical course and the role of active surgical treatment. Neurosurgery 2004;54:840–844.

Tsuyoshi Ohta, M.D.
Department of Neurosurgery, Graduate School of Medicine, Kyoto University, Kyoto, Japan

Ken-ichiro Kikuta, M.D., Ph.D.
Department of Neurosurgery, Graduate School of Medicine, Kyoto University, Kyoto, Japan

Hirotoshi Imamura, M.D.
Department of Neurosurgery, Graduate School of Medicine, Kyoto University, Kyoto, Japan

Yasushi Takagi, M.D., Ph.D.
Department of Neurosurgery, Graduate School of Medicine, Kyoto University, Kyoto, Japan

Masaki Nishimura, M.D., Ph.D.
Department of Neurosurgery, Graduate School of Medicine, Kyoto University, Kyoto, Japan

Yoshiki Arakawa, M.D., Ph.D.
Department of Neurosurgery, Graduate School of Medicine, Kyoto University, Kyoto, Japan

Nobuo, Hashimoto, M.D., Ph.D.
Department of Neurosurgery, Graduate School of Medicine, Kyoto University, Kyoto, Japan

Kazuhiko Nozaki, M.D., Ph.D.
Department of Neurosurgery, Graduate School of Medicine, Kyoto University, Kyoto, Japan

Reprint requests:
Ken-ichiro Kikuta, M.D., Ph.D., Department of Neurosurgery, Graduate School of Medicine, Kyoto University, 54 Kawaharacho, Shogoin, Sakyo-ku, Kyoto 606-8507, Japan.
Email: kikuta@kuhp.kyoto-u.ac.jp

Received, October 24, 2005.
Accepted, May 10, 2006.

ADMINISTRATION OF EX VIVO-EXPANDED BONE MARROW-DERIVED ENDOTHELIAL PROGENITOR CELLS ATTENUATES FOCAL CEREBRAL ISCHEMIA-REPERFUSION INJURY IN RATS

OBJECTIVE: This study aimed to examine early effects of ex vivo-expanded bone marrow-derived endothelial progenitor cells (EPCs) on focal cerebral ischemia-reperfusion injury.

METHODS: EPCs were obtained from mononuclear cells of autologous bone marrow of a rat. After culture on fibronectin-coated dishes for 10 to 14 days, 2.5×10^5 cells of EPCs were administered transarterially after 90 minute occlusion of the middle cerebral artery.

RESULTS: Administration of EPCs significantly reduced both the infarct volume and the scores of neurological deficits at 24 and 48 hours. EPCs administered 2 hours after insult did not reduce infarct volume, but attenuated neurological deficits at 24 hours. Administration of EPCs significantly reduced the number of myeloperoxidase-immunoreactive cells in the ischemic lesion at 24 hours and increased regional cortical blood flow at 48 hours. EPCs were observed in the ischemic hemisphere and around the endothelial layer of the pial arteries. Most of them expressed endothelial nitric oxide synthase.

CONCLUSION: Administration of ex vivo-expanded bone marrow-derived EPCs reduced infarct volume and neurological deficits in acute focal brain ischemia-reperfusion injury caused, at least in part, by attenuation of endothelial dysfunction.

KEY WORDS: Cerebral infarction, Endothelial dysfunction, Endothelial progenitor cells

Neurosurgery 59:679-686, 2006 DOI: 10.1227/01.NEU.0000229058.08706.88 www.neurosurgery-online.com

Endothelial progenitor cells (EPCs) were first discovered in the leukocyte fraction of human peripheral blood that expressed CD34 on the cell surface (2). EPCs can be isolated from umbilical cord blood, peripheral blood, or bone marrow (BM) (3, 5, 19, 26). Mobilization of EPCs from BM to peripheral blood is enhanced in pathological conditions such as tissue ischemia, wound healing, and focal cerebral ischemia for promoting local angiogenesis (1, 2, 34, 37). Local injection of ex vivo-expanded EPCs can reduce hind limb ischemia and myocardial infarction (19, 20). Beneficial effects of EPCs on focal cerebral ischemia in the chronic stage were reported (37), but early effects have not been fully clarified. In this study, we focused on the early effects of transarterial administration of ex vivo-expanded BM-derived EPCs on focal cerebral ischemia-reperfusion injury.

METHODS

Animals

All procedures were performed in accordance with the guidelines of the Animal Research Committee of Kyoto University Graduate School of Medicine. Male Sprague-Dawley rats weighing 280 to 300 g (age, 8–10 wk) were obtained from Shimizu Laboratory Supplies Co., Ltd. (Kyoto, Japan).

Preparation of BM-derived EPCs

EPCs were obtained from autologous BM of rats (22). BM was aspirated from the shaft of the femur under general anesthesia with halothane. Mononuclear cell fractions were isolated by centrifugation with Ficoll-Paque density gradient (Pharmacia, Uppsala, Sweden) (19, 26). Cells were resuspended in endothelial

cell (EC) basal medium-2 (Cambrex Corp., East Rutherford, NJ) plus microvascular endothelial cell medium-2 SingleQuots containing 5% fetal bovine serum, human vascular endothelial growth factor (VEGF)-1, human fibroblast growth factor-2, human epidermal growth factor, insulin-like growth factor (IGF)-1, and ascorbic acid and cultured on a fibronectin-coated dish (Biocoat, Fort Washington, PA) at 37°C under 5% carbon dioxide. On Day 4, nonadherent cells were removed, and adherent cells were cultured and maintained 6 to 10 more days.

Cellular Staining

On Day 10, cultured cells were incubated with 1,1'-dioctadecyl-3,3,3',3'-tetramethylindocarbocyanine-labeled acetylated low-density lipoprotein (acLDL) (1:200; Molecular Probes, Eugene, OR) at 37°C for 4 hours and fixed with 4% phosphate-buffered paraformaldehyde (PBPA) for 10 minutes. Later, they were reacted with fluorescein isothiocyanate-conjugated *Bandeiraea simplicifolia* isolectin B4 (Sigma-Aldrich, St. Louis, MO) or with mouse monoclonal antibodies against von Willebrand Factor (vWF) (DAKO, Glostrup, Denmark) at 37°C for 4 hours (35).

Immunoblotting

Immunoblotting with rabbit polyclonal antibodies against Flk-1 (NeoMarkers, Fremont, CA), Tie-2 (Sigma-Aldrich), goat polyclonal antibody against intracellular adhesion molecule (ICAM)-1(Sigma-Aldrich), mouse monoclonal antibodies against vWF (DAKO), or α-tubulin (Sigma-Aldrich) was performed on the cells on Day 10, and with human microvascular ECs (Cambrex) and human aortic smooth muscle cells (Cambrex), as previously reported (18).

Transient Middle Cerebral Artery Occlusion of Rats and Transarterial Administration of EPCs

Methods for the preparation of a rat middle cerebral artery (MCA) occlusion model were described in our previous reports (4, 13, 14, 27, 30, 31, 32, 33). In the preliminary experiments, physiological parameters, including blood pressure and blood gas data, had been stabilized in the model to make the infarct volume stable and reproductive (4). Some modifications were added to a thread for arterial occlusion (23, 24). The thread consisted of a nylon monofilament and a polyethylene tube. Thirty-eight millimeters of 3–0 nylon monofilament was passed through a 15-mm polyethylene tube (inner diameter, 0.28 mm; outer diameter, 0.61 mm) (Natume, Tokyo, Japan). Both tails of the monofilament and the tube were fixed to each other with silicone (Heraeus Kulzer, Hanau, Germany). Thus, the tip of the thread consisted of a bare nylon monofilament (*Fig. 1G*). After surgical exposure and temporary occlusion of the common carotid artery and the internal carotid artery (ICA), the tip of the thread was navigated into the ICA through the external carotid artery (length, 19 mm). When the tip of the thread reached the top of the ICA, the tube was also introduced into the ICA proximal to the pterygopalatine artery (*Fig. 1G*). After 90-minute occlusion, only the nylon filament was withdrawn, and the tube remained within the ICA. Autologous EPCs on Day 10 of 2.5×10^5 suspended in 0.3 ml phosphate-buffered saline (PBS (-)) were injected into the ICA through the tube in 60 seconds. In the delayed group, EPCs were injected 2 hours after the reperfusion. The filament was completely withdrawn, and the stump of the external carotid artery was clipped for 2 hours without heparin. After that, only the tube was introduced into the ICA. After discontinuation of halothane, the rats recovered spontaneously. In the control rats, 0.3 ml PBS (-) or A10 (embryonic thoracic aorta, smooth muscle, DB1X

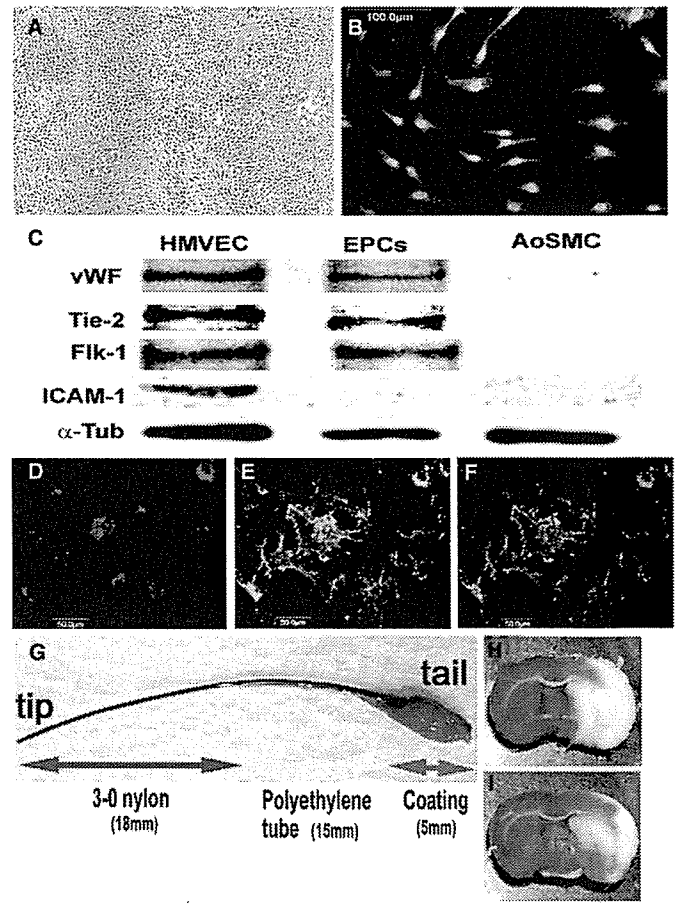

FIGURE 1. *Molecular characterization of EPCs and rat MCA occlusion model. Cells cultured for 10 days showed a typical cobblestone appearance* (A) *and expressed vWF* (B). C, *immunoblottings demonstrating vWF, Tie-2, Flk-1, and α-tubulin expression, but not ICAM-1. They incorporated 1,1'-dioctadecyl-3,3,3',3'-tetramethylindocarbocyanine-acLDL* (D) *and bound to fluorescein isothiocyanate-labeled lectin* (E) *and* (F), *merged.* Scale bars = *100 μm* (B) *and 50 μm* (D–F). G, *the thread for MCA occlusion was provided as a 38-mm 3–0 nylon monofilament passing through a 15-mm polyethylene tube (inner diameter, 0.28 mm; outer diameter, 0.61 mm) with its tail fixed to itself by silicone. The infarct lesion was defined as sparing site from 2,3,5-triphenyltetrazolium chloride staining. Representative photographs of lesion at 48 hours in control* (H) *and EPC* (I) *groups.*

rat) (Dainippon Pharmaceutical Co., Ltd., Osaka, Japan) was injected. During the entire procedure, the rectal temperature was kept between 36.5 and 37.0°C with a heating pad.

Evaluation of Infarct Volume

Rats were deeply anesthetized with diethyl ether for 3 minutes at 24 or 48 hours. After decapitation, brains were quickly extracted, and coronal sections (thickness, 2 mm) were immersed in a 2% solution of 2,3,5-triphenyltetrazolium chloride (Sigma-Aldrich) in PBS (-) at 37°C for 30 minutes (28). They were digitally photographed, and the infarct volume was calculated using SCION imager (Scion Corp., Frederick, MD) (10). Infarct volume was expressed as the ratio of it to the volume of contralateral hemisphere in the same individual.

Evaluation of Neurological Deficits

Motor function was evaluated at 24 or 48 hours with a walking trial on the rotating spindle of a Rota rod (Muromachi, Tokyo, Japan) (23). Rats were preconditioned to walk on the spindle at a constant speed of 2, 4, 6, and 8 revolutions per minute (rpm) until they were able to stay on it for 120 seconds. Thereafter, the rotating speed was set to increase to 40 rpm in 300 seconds, and the rpm at the time of falling was defined as the function score (12).

Immunohistochemical Analysis of In Vivo Distribution of EPCs

Adenoviral vector for expression of green fluorescent protein (GFP, 4×10^7 PFU/ml, 2 multiplicity of infection) was transfected to EPCs on Day 8 (11) and administered to MCA occlusion or sham-operated rats 2 days after transfection. Extensive expression of GFP on EPCs between 24 to 72 hours later was confirmed in vitro (data not shown). Rats were perfused with PBS (-) and 4% PBPA under deep anesthesia at 24 and 48 hours and fixed with 4% PBPA for 24 hours and 0.5 mol/L sucrose for another 24 hours. Frozen coronal sections (thickness, 10 μm) from the center of the ischemic lesion at the level of the anterior commissure (interaural, 8.2 mm; bregma, 0.8 mm) were embedded in optimal cutting temperature compound (Sakura Finetechnical, Tokyo, Japan) and stained with mouse monoclonal antibodies against vWF (DAKO) or α-smooth muscle actin (NeoMarkers). The relationships between EPCs and ICAM-1, VEGF, eNOS, and IGF-1 were examined in the paraffin-embedded 10-μm thick sections. After deparaffinization (xylen, 10 min; absolute alcohol, 10 min; 95% alcohol, 3 min; 70% alcohol, 3 min), they were stained with rabbit polyclonal and mouse monoclonal antibodies against GFP (Molecular Probes) and mouse monoclonal antibodies against ICAM-1 (Santa Cruz Biotechnology, Inc., Santa Cruz, CA), rabbit polyclonal antibodies against VEGF and eNOS (Lab Vision, Fremont, CA) ,and mouse monoclonal antibody against IGF-1 (Upstate, Charlottesville, VA). Then, they were reacted with goat antimouse monoclonal or rabbit polyclonal antibodies conjugating Alexa Fluor Dye (Molecular Probes) of each spectrum 488, 546, and 647. The confocal laser scanning microscope (Fluoview, FV300, Olympus, Japan) was used in this study.

Measurement of Regional Cerebral Cortical Blood Flow

Regional cerebral cortical blood flow (rCoBF) at the same point of the brain surface was measured as previously reported, with modification (7). The dural surface in the right parietal cortex located at 2 mm lateral and 1 mm caudal to bregma (*Fig. 3A*) was surgically exposed under halothane, which was considered MCA territory around the ischemic core (24). A laser Doppler flowmeter probe (Flo-C1, Omegawave, Tokyo, Japan) was placed and fixed tightly with resin. On that day, transient MCA occlusion and EPC administration were performed. rCoBF was measured sequentially just before insult and at 24 and 48 hours under halothane (8, 33). The

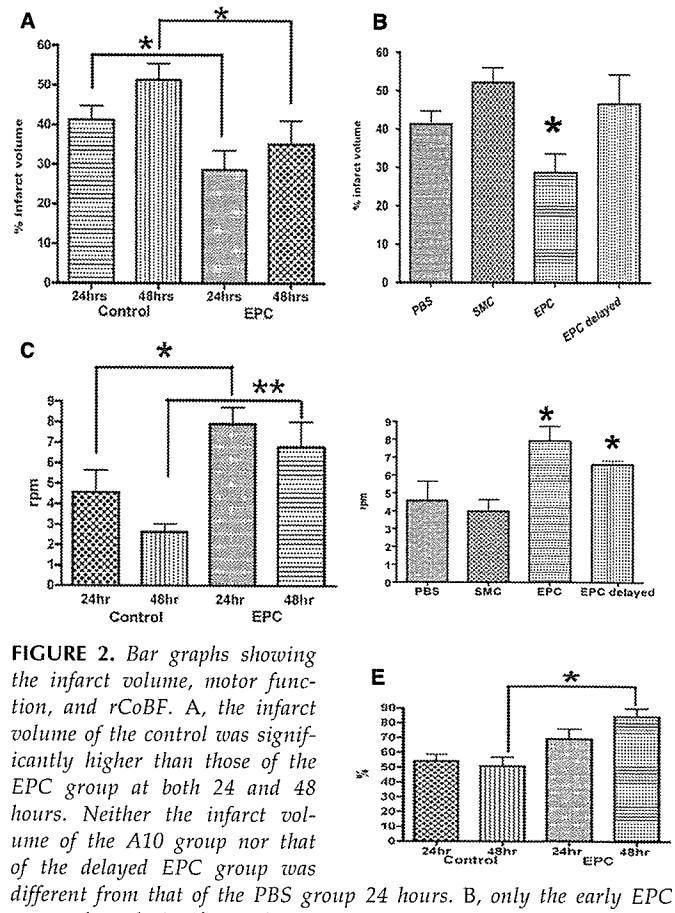

FIGURE 2. *Bar graphs showing the infarct volume, motor function, and rCoBF.* A, *the infarct volume of the control was significantly higher than those of the EPC group at both 24 and 48 hours. Neither the infarct volume of the A10 group nor that of the delayed EPC group was different from that of the PBS group 24 hours.* B, *only the early EPC group showed significant decrement.* C, *the motor function scores of the EPC group were significantly higher than the control both at 24 and 48 hours.* D, *both the early and delayed EPC groups showed significant improvement at 24 hours after ischemia in comparison with the A10 and PBS groups.* E, *rCoBF was significantly higher in the EPC group than in the control at 48 hours.* Single asterisk, $P < 0.05$; double asterisk, $P < 0.01$.

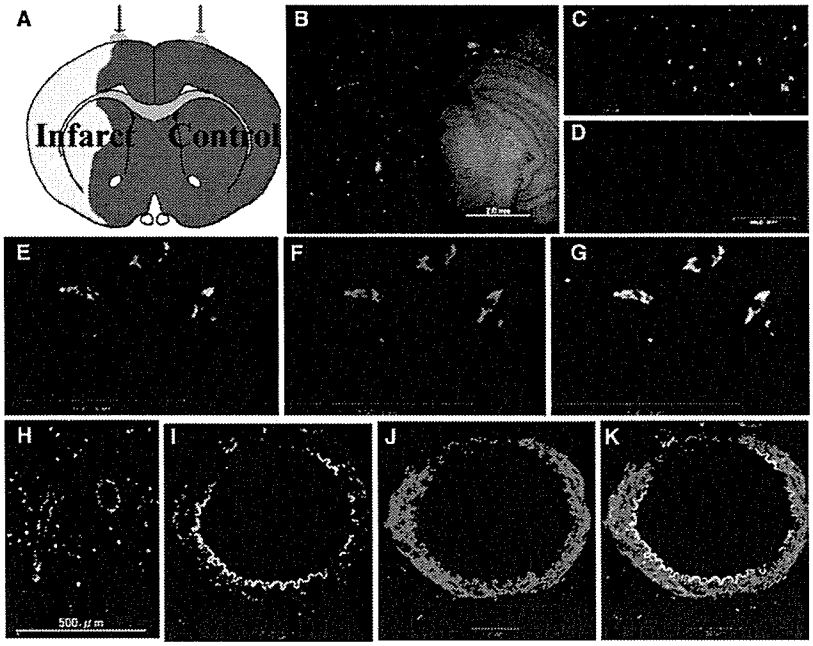

FIGURE 3. *Distribution of administrated EPCs. rCoBF was measured at 2 mm lateral and 1 mm caudal to the bregma.* A, *immunohistochemical evaluation was performed in the symmetrical regions of the lateral cortex, including the infarct and noninfarct regions, at 24 hours.* B, *EPCs expressing GFP were mainly distributed in the ischemic hemisphere. Although few cells expressing GFP were observed in the contralateral hemisphere* (B, *lower magnification;* D, *higher magnification), many of them were widely observed in the brain parenchyma of the ischemic side* (B, *lower magnification;* C, *higher magnification) with expression of vWF at 24 hours* (F *and* G, *merged).* H, *EPCs were also distributed in the inner layers of many arteries in the ischemic lesion. They were located medial to the smooth muscle layer* (I), *which was demonstrated by staining with α-smooth muscle actin* (J *and* K *are merged).* Scale bars = 2 *mm* (B), *200 μm* (C *and* D), *100 μm* (E–G), *500 μm* (H), *50 μm* (I—K).

rectal temperature was kept between 36.5 and 37.0°C. Its change was expressed as the ratio to the preoperative value.

Infiltration of Myeloperoxidase-immunoreactive Cells

Rats were perfused with PBS (-) and 4% PBPA under deep anesthesia at 24 hours. A 10-μm thick frozen coronal section from the center of the ischemic lesion at the level of the anterior commissure was stained with polyclonal rabbit anti-human myeloperoxidase (MPO) antibody (DAKO) to count the number of inflammatory neutrophils. The density of MPO-immunoreactive cells throughout the whole infarct region was expressed by the number counted at ×400 magnification per infarct area (cells/mm^2).

Statistical Analysis

Data were expressed as mean and standard deviations for the given number of animals and statistically evaluated using the unpaired Student's *t* test. Differences were accepted as being significant at a *P* value less than 0.05.

RESULTS

Molecular Characteristics of BM-derived EPCs

BM-derived mononuclear cells showed a cobblestone appearance similar to ECs (*Fig. 1A*) with expression of vWF (*Fig. 1B*). Immunoblotting revealed expression of Tie-2, Flk-1, and vWF, which are specifically expressed in ECs. However, they did not express ICAM-1 (*Fig. 1C*). They endocyted 1,1'-dioctadecyl-3,3,3',3'-tetramethylindocarbocyanine-labeled acLDL (*Fig. 1D*) and were bound to fluorescein isothiocyanate-labeled isolectin B4, which is a murine-specific surface marker of ECs (*Fig. 1, E* and *F*) (19).

Infarct Volume

Ninety-minute occlusion of MCA induced a large cerebral infarct, including the whole caudoputamen and part of the lateral cortex. The infarct volume of the PBS group (*Fig. 1H*) and the EPC group (*Fig. 1I*) was 41.3 ± 10.5% (n = 9) and 28.7 ± 13.8% (n = 8), respectively, at 24 hours. The volume of each group at 48 hours was 51.4 ± 12.2% (n = 9) and 35.1 ± 16.7% (n = 8), respectively. The infarct volumes both at 24 and 48 hours were significantly lower in the EPC group than in the control ($P < 0.05$) (*Fig. 2A*). The infarct volume at 24 hours of the A10 transplanted and delayed EPC groups was 52.2 ± 11.6% (n = 9) and 46.5 ± 13.3% (n = 3), respectively. Only the early EPC group showed a significant reduction of infarct volume ($P < 0.05$) (*Fig. 3B*).

Neurological Deficits

Motor function scores of the PBS and EPC groups were 4.57 ± 2.84 (n = 7) and 7.91 ± 2.45 rpm (n = 9), respectively, at 24 hours and 2.61 ± 1.15 (n = 8) and 6.79 ± 3.46 rpm (n = 8), respectively, at 48 hours. The score of the EPC group was significantly higher than that of the control at both 24 and 48 hours ($P < 0.05$ at 24 hr, $P < 0.01$ at 48 hr) (*Fig. 3C*). The motor function scores of the A10 and delayed EPC groups at 24 hours were 4.0 ± 1.91 (n = 9) and 6.6 ± 0.36 rpm (n = 3), respectively. Delayed EPC group showed significant improvement ($P < 0.05$) (*Fig. 3D*).

rCoBF

The value of rCoBF of the control (n = 5) was decreased to 54.2 ± 10.2% of the preoperative value at 24 hours and remained 50.6 ± 13.7% at 48 hours. The value of rCoBF of the EPC group (n = 5) was decreased to 68.9 ± 15.3% at 24 hours, but recovered to 84.4 ± 12.0% at 48 hours. The value of rCoBF in the EPC group at 48 hours was significantly higher than that of the control ($P < 0.05$) (*Fig. 3E*).

Distribution of Administrated EPCs

Distribution of EPCs was estimated in the similar lateral cortex (*Fig. 3A*). Although few cells expressing GFP were observed in the contralateral hemisphere (*Fig. 3, B* and *D*), many were observed widely in the ischemic brain parenchyma (*Fig. 3, B* and *C*) with expression of vWF at 24 hours (*Fig. 3, E–G*). EPCs seemed to replace the endothelial layer entirely in some arteries (*Fig. 3H*). They were located medial to the smooth muscle layer (*Fig. 3, I–K*). These observations were also confirmed at 48 hours. In the rats in which EPCs were administered without ischemic insult, few cells expressing GFP were observed in the brain (data not shown).

Density of MPO-immunoreactive Cells

Administration of EPCs significantly reduced the infiltration of MPO-immunoreactive cells in the ischemic hemisphere at 24 hours ($P < 0.05$) (*Fig. 4A*). The density of the MPO-immunoreactive cells in the ischemic hemisphere at 24 hours was 37.4 ± 14.0 cells/mm^2 (control, n = 4, *Fig. 4B*) and 15.3 ± 3.95 cells/mm^2 (EPCs, n = 4, *Fig. 4C*). ICAM-1 positive cells were distributed throughout the ischemic hemisphere, but its expression was not colocalized with the transplanted EPCs (*Fig. 4, D–F*).

Expression of eNOS, VEGF, and IGF-1 in Administered EPCs

Administered EPCs expressing GFP were distributed in the brain parenchyma and around the endothelial layer of pial arteries in the ischemic lesions at 24 hours (*Fig. 5, A, D,* and *G*). Most of the cells also expressed eNOS (*Fig. 5, B* and *C*). Expression of VEGF (*Fig. 5, E* and *F*) and IGF-1 (*Fig. 5, H* and *I*) was mainly observed in the cells other than EPCs in the ischemic lesion.

DISCUSSION

EPCs can be isolated from peripheral blood, BM, and umbilical cord blood (3, 5, 19, 26). In this study, we used EPCs obtained from autologous BM by culture with VEGF on fibronectin-coated dishes by removing the nonadherent cells because this method seemed to provide more purified EPCs than culture of freshly isolated CD34-positive cells (26). Molecular characteristics of EPCs isolated and expanded from BM were similar to that of vascular ECs, such as uptake of acLDL, binding to lectin, and expression of vWF, Flk-1, and Tie-2, except for the expression of ICAM-1.

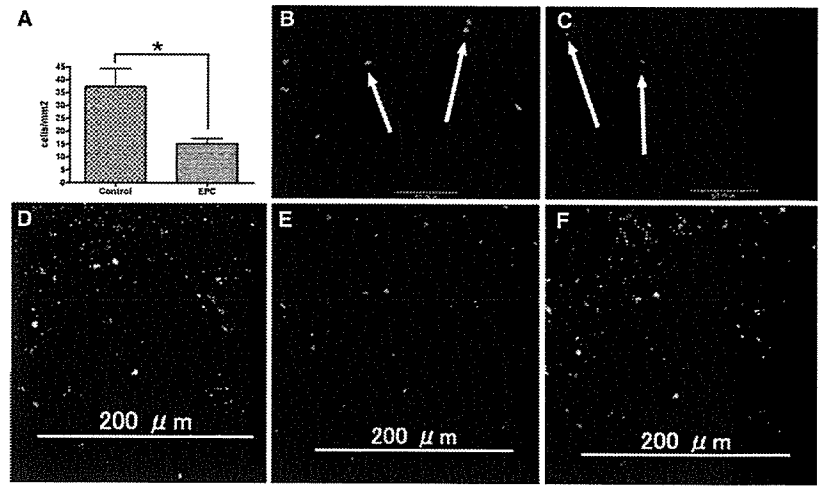

FIGURE 4. *Density of the MPO-immunoreactive cells in the ischemic lesion.* A, *the density of the MPO-immunoreactive cells in the ischemic hemisphere at 24 hours was significantly reduced by administration of EPCs ($P < 0.05$). MPO-immunoreactive cells* (arrows) *in the control* (B) *and EPC group* (C). *ICAM-1 positive cells* (D) *and EPCs* (E) *were distributed throughout the ischemic hemisphere. Their distribution differed* (F, *merged*). Scale bars = *200 μm.*

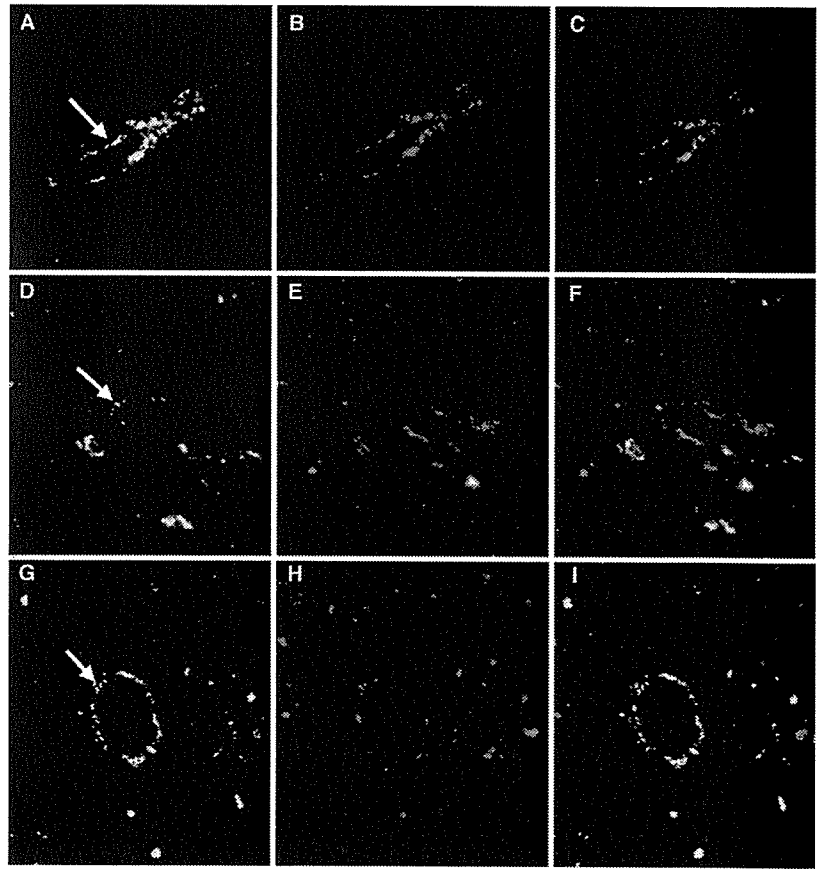

FIGURE 5. *Expression of eNOS, VEGF, and IGF-1 in administered EPCs.* A, D, *and* G, *administered EPCs expressing GFP were distributed in the brain parenchyma and around the endothelial layer of pial arteries in the ischemic lesions at 24 hours. Most of the cells also expressed eNOS* (B *and* C *are merged). Expression of VEGF* (E *and* F *are merged) and IGF-1* (H *and* I *are merged) was observed in the cells other than EPCs in the ischemic lesion.*

Administration of ex vivo-expanded BM-derived EPCs could reduce the cerebral infarct volume and the neurological deficits at 24 and 48 hours after focal cerebral ischemia-reperfusion injury. rCoBF was reduced after ischemia, but significantly recovered by administration of EPCs at 48 hours. Delayed administration also showed partial beneficial effects on the ischemia.

To investigate the mechanism of the beneficial effects of EPCs at 24 hours, we focused on the cellular interactions between EPCs and inflammatory neutrophils. Endothelial dysfunction has been reported to be significantly involved in neural injury after focal cerebral ischemia-reperfusion injury (6), and MPO-immunoreactive cells are regarded as a general marker of acute endothelial damage. Infiltration of MPO-positive cells is initiated within a few hours after insult because of the interaction with ECs of enhanced expression of ICAM-1 (6, 21, 25). Administration of EPCs actually suppressed the infiltration of MPO-immunoreactive cells in the infarct region. Although EPCs were assembled widely in the parenchyma of the ischemic hemisphere, and especially in the inner layer of several pial arteries at 24 hours, distribution of EPCs was different from that of ICAM-1 positive cells. We think that lack of expression of ICAM-1 on the surface of the EPCs might be related to the inhibitory effects.

rCoBF in the ischemic penumbra was reduced at 24 hours after ischemia, but significantly recovered by administration of EPCs at 48 hours. Attenuation of infarct volume and neurological deficit at 48 hours might be related to the recovery of rCoBF.

To investigate the molecular mechanisms in attenuation of acute ischemic injury by administration of EPCs, we carried out an immunohistochemical study of expression of eNOS, VEGF, and IGF-1 in the EPCs. EPCs were reported to produce several vasodilatory or growth factors such as nitric oxide, VEGF, and IGF-1 (15). Most of the EPCs distributed in the ischemic lesion expressed eNOS, but few expressed VEGF and IGF-1. These observations suggest that nitric oxide produced by EPCs might be related to the attenuation of endothelial dysfunction or ischemic injury (9, 16, 36).

Zhang et al. (37) reported focal brain ischemia mobilized EPCs from BM to ischemic lesions at 30 days after insult. They were differentiated into ECs in the ischemic region participating in the neovascularization with recovery of cerebral blood flow. Our study revealed that exogenously administered EPCs assembled widely in the parenchyma of the ischemic hemisphere and in the inner layer of several pial arteries with endothelial differentiation, even in the acute ischemic stage. Endothelial differentiation in the ischemic region might occur earlier in the exogenous EPCs than endogenous ones from the BM. This is clinically important in that exogenously administrated EPCs might have therapeutic potential for acute brain ischemia.

Although Taguchi et al. (29) reported beneficial effects of CD34-positive cells derived from human umbilical cord on mouse focal brain ischemia, their method needs immunosuppression for clinical application. Iihoshi et al. (17) reported beneficial effects of administration of stromal cells from autologous BM for focal ischemia, but the target of cells or molecules in their method remains somewhat ambiguous because stromal cells have multipotency. Our method also has some limitations to be solved for clinical application. Delayed administration of EPCs had partial effects on ischemia in our study. In addition, our method takes several days for differentiation of the cells before administration. However, relief of endothelial dysfunction by administration of expanded autologous EPCs will be another possible therapeutic option in the treatment of acute brain ischemia.

CONCLUSION

In summary, administration of ex vivo-expanded autologous BM-derived EPCs diminished the early neural injury after focal cerebral ischemia-reperfusion injury. This might be caused, in part, by attenuation of acute inflammatory endothelial dysfunction.

REFERENCES

1. Asahara T, Masuda H, Takahashi T, Kalka C, Pastore C, Silver M, Kearne M, Magner M, Isner JM: Bone marrow origin of endothelial progenitor cells responsible for postnatal vasculogenesis in physiological and pathological neovascularization. **Circ Res** 85:221–228, 1999.
2. Asahara T, Murohara T, Sullivan A, Silver M, van der Zee R, Li T, Witzenbichler B, Schatteman G, Isner JM: Isolation of putative progenitor endothelial cells for angiogenesis. **Science** 275:964–967, 1997.
3. Asahara T, Takahashi T, Masuda H, Kalka C, Chen D, Iwaguro H, Inai Y, Silver M, Isner JM: VEGF contributes to postnatal neovascularization by mobilizing bone marrow-derived endothelial progenitor cells. **EMBO J** 18: 3964–3972, 1999.
4. Asahi M, Hoshimaru M, Uemura Y, Tokime T, Kojima M, Ohtsuka T, Matsuura N, Aoki T, Shibahara K, Kikuchi H: Expression of interleukin-1 beta converting enzyme gene family and bcl-2 gene family in the rat brain following permanent occlusion of the middle cerebral artery. **J Cereb Blood Flow Metab** 17:11–18, 1997.
5. Boyer M, Townsend LE, Vogel LM, Falk J, Reitz-Vick D, Trevor KT, Villalba M, Bendick PJ, Glover JL: Isolation of endothelial cells and their progenitor cells from human peripheral blood. **J Vasc Surg** 31:181–189, 2000.
6. Connolly ES Jr, Winfree CJ, Springer TA, Naka Y, Liao H, Yan SD, Stern DM, Solomon RA, Gutierrez-Ramos JC, Pinsky DJ: Cerebral protection in homozygous null ICAM-1 mice after middle cerebral artery occlusion. Role of neutrophil adhesion in the pathogenesis of stroke. **J Clin Invest** 97:209–216, 1996.
7. Ding Y, Li J, Rafols JA, Phillis JW, Diaz FG: Prereperfusion saline infusion into ischemic territory reduces inflammatory injury after transient middle cerebral artery occlusion in rats. **Stroke** 33:2492–2498, 2002.
8. Dogan A, Rao AM, Hatcher J, Rao VL, Baskaya MK, Dempsey RJ: Effects of MDL 72527, a specific inhibitor of polyamine oxidase, on brain edema, ischemic injury volume, and tissue polyamine levels in rats after temporary middle cerebral artery occlusion. **J Neurochem** 72:765–770, 1999.
9. Fagan KA, Fouty BW, Tyler RC, Morris KG Jr, Hepler LK, Sato K, LeCras TD, Abman SH, Weinberger HD, Huang PL, McMurtry IF, Rodman DM: The pulmonary circulation of homozygous or heterozygous eNOS-null mice is hyperresponsive to mild hypoxia. **J Clin Invest** 103:291–299, 1999.
10. Furuya K, Kawahara N, Kawai K, Toyoda T, Maeda K, Kirino T: Proximal occlusion of the middle cerebral artery in C57Black6 mice: Relationship of patency of the posterior communicating artery, infarct evolution, and animal survival. **J Neurosurg** 100:97–105, 2004.
11. Furuyashiki T, Arakawa Y, Takemoto-Kimura S, Bito H, Narumiya S: Multiple spatiotemporal modes of actin reorganization by NMDA receptors and voltage-gated Ca2+ channels. **Proc Natl Acad Sci U S A** 99:1458–1463, 2002.

12. Gupta YK, Sinha K, Chaudhary G: Transient focal ischemia induces motor deficit but does not impair the cognitive function in middle cerebral artery occlusion model of stroke in rats. **J Neurol Sci** 203:267–271, 2002.
13. Hattori I, Takagi Y, Nakamura H, Nozaki K, Bai J, Kondo N, Sugino T, Nishimura M, Hashimoto N, Yodoi J: Intravenous administration of thioredoxin decreases brain damage following transient focal cerebral ischemia in mice. **Antioxid Redox Signal** 6:81–87, 2004.
14. Hayashi J, Takagi Y, Fukuda H, Imazato T, Nishimura M, Fujimoto M, Takahashi J, Hashimoto N, Nozaki K: Primate embryonic stem cell-derived neuronal progenitors transplanted into ischemic brain. **J Cereb Blood Flow Metab** Jan 4, 2006 [Epub ahead of print].
15. Hristov M, Weber C: Endothelial progenitor cells: Characterization, pathophysiology, and possible clinical relevance. **J Cell Mol Med** 8:498–508, 2004.
16. Huang Z, Huang PL, Ma J, Meng W, Ayata C, Fishman MC, Moskowitz MA: Enlarged infarcts in endothelial nitric oxide synthase knockout mice are attenuated by nitro-L-arginine. **J Cereb Blood Flow Metab** 16:981–987, 1996.
17. Iihoshi S, Honmou O, Houkin K, Hashi K, Kocsis JD: A therapeutic window for intravenous administration of autologous bone marrow after cerebral ischemia in adult rats. **Brain Res** 1007:1–9, 2004.
18. Ikeda H, Yamaguchi M, Sugai S, Aze Y, Narumiya S, Kakizuka A: Expanded polyglutamine in the Machado-Joseph disease protein induces cell death in vitro and in vivo. **Nat Genet** 13:196–202, 1996.
19. Kalka C, Masuda H, Takahashi T, Kalka-Moll WM, Silver M, Kearney M, Li T, Isner JT, Asahara T: Transplantation of ex vivo expanded endothelial progenitor cells for therapeutic neovascularization. **Proc Natl Acad Sci U S A** 97:3422–3427, 2000.
20. Kawamoto A, Tkebuchava T, Yamaguchi J, Nishimura H, Yoon YS, Milliken C, Uchida S, Masuo O, Iwaguro H, Ma H, Hanley A, Silver M, Kearney M, Losordo DW, Isner JM, Asahara T: Intramyocardial transplantation of autologous endothelial progenitor cells for therapeutic neovascularization of myocardial ischemia. **Circulation** 107:461–468, 2003.
21. Kitagawa K, Matsumoto M, Mabuchi T, Yagita Y, Ohtsuki T, Hori M, Yanagihara T: Deficiency of intercellular adhesion molecule 1 attenuates microcirculatory disturbance and infarction size in focal cerebral ischemia. **J Cereb Blood Flow Metab** 18:1336–1345, 1998.
22. Knaan-Shanzer S, Houben P, Kinwel-Bohre EP, van Bekkum DW: Remission induction of adjuvant arthritis in rats by total body irradiation and autologous bone marrow transplantation. **Bone Marrow Transplant** 8:333–338, 1991.
23. Kuroda S, Tsuchidate R, Smith ML, Maples KR, Siesjo BK: Neuroprotective effects of a novel nitrone, NXY-059, after transient focal cerebral ischemia in the rat. **J Cereb Blood Flow Metab** 19:778–787, 1999.
24. Longa EZ, Weinstein PR, Carlson S, Cummins R: Reversible middle cerebral artery occlusion without craniectomy in rats. **Stroke** 20:84–91, 1989.
25. Reynolds GM, Young FI, Young JA, Williams A, Rowlands DC: Microwave oven antigen retrieval applied to the immunostaining of cytopathology specimens. **Cytopathology** 5:345–358, 1994.
26. Shintani S, Murohara T, Ikeda H, Ueno T, Sasaki K, Duan J, Imaizumi T: Augmentation of postnatal neovascularization with autologous bone marrow transplantation. **Circulation** 103:897–903, 2001.
27. Sugino T, Nozaki K, Takagi Y, Hattori I, Hashimoto N, Yodoi J: Expression and distribution of redox regulatory protein, thioredoxin after metabolic impairment by 3-nitropropionic acid in rat brain. **Neurosci Lett** 275:145–148, 1999.
28. Sun Y, Jin K, Xie L, Childs J, Mao XO, Logvinova A, Greenberg DA: VEGF-induced neuroprotection, neurogenesis, and angiogenesis after focal cerebral ischemia. **J Clin Invest** 111:1843–1851, 2003.
29. Taguchi A, Soma T, Tanaka H, Kanda T, Nishimura H, Yoshikawa H, Tsukamoto Y, Iso H, Fujimori Y, Stern DM, Naritomi H, Matsuyama T: Administration of CD34+ cells after stroke enhances neurogenesis via angiogenesis in a mouse model. **J Clin Invest** 114:330–338, 2004.
30. Takagi Y, Horikawa F, Nozaki K, Sugino T, Hashimoto N, Yodoi J: Expression and distribution of redox regulatory protein, thioredoxin during transient focal brain ischemia in the rat. **Neurosci Lett** 251:25–28, 1998.
31. Takagi Y, Nakamura T, Nishiyama A, Nozaki K, Tanaka T, Hashimoto N, Yodoi J: Localization of glutaredoxin (thioltransferase) in the rat brain and possible functional implications during focal ischemia. **Biochem Biophys Res Commun** 258:390–394, 1999.
32. Takagi Y, Nishimura M, Morizane A, Takahashi J, Nozaki K, Hayashi J, Hashimoto N: Survival and differentiation of neural progenitor cells derived from embryonic stem cells and transplanted into ischemic brain. **J Neurosurg** 103:304–310, 2005.
33. Takagi Y, Tokime T, Nozaki K, Gon Y, Kikuchi H, Yodoi J: Redox control of neuronal damage during brain ischemia after middle cerebral artery occlusion in the rat: Immunohistochemical and hybridization studies of thioredoxin. **J Cereb Blood Flow Metab** 18:206–214, 1998.
34. Takahashi T, Kalka C, Masuda H, Chen D, Silver M, Kearney M, Magner M, Isner JM, Asahara T: Ischemia- and cytokine-induced mobilization of bone marrow-derived endothelial progenitor cells for neovascularization. **Nat Med** 5:434–438, 1999.
35. Walter DH, Rittig K, Bahlmann FH, Kirchmair R, Silver M, Murayama T, Nishimura H, Losordo DW, Asahara T, Isner JM: Statin therapy accelerates reendothelialization: a novel effect involving mobilization and incorporation of bone marrow-derived endothelial progenitor cells. **Circulation** 105: 3017–3024, 2002.
36. White RP, Deane C, Vallance P, Markus HS: Nitric oxide synthase inhibition in humans reduces cerebral blood flow but not the hyperemic response to hypercapnia. **Stroke** 29:467–472, 1998.
37. Zhang ZG, Zhang L, Jiang Q, Chopp M: Bone marrow-derived endothelial progenitor cells participate in cerebral neovascularization after focal cerebral ischemia in the adult mouse. **Circ Res** 90:284–288, 2002.

Acknowledgments

This work was supported by Grants-in-Aid for Scientific Research from the Japanese Society for the Promotion of Science. Adenoviral vector for expression of green fluorescent protein was kindly provided by Professor Shuh Narumiya (Department of Pharmacology, Kyoto University Graduate School of Medicine).

COMMENTS

The authors demonstrate neuroprotection and improved functional outcome in the acute phase of reperfused stroke after an intra-arterial injection of ex vivo expanded bone marrow endothelial progenitor cells. They propose that this neuroprotection derives from an attenuation of endothelial dysfunction, reflected by a reduction in the density of myeloperoxidase-positive cells in the area of the infarction and an increase in regional blood flow, assessed by laser Doppler flowmetry from 24 to 48 hours in the treated animals. Although previous work has demonstrated that endothelial progenitor cells (EPCs) ameliorate functional outcome in the chronic phase of stroke, this is the first study to assess functional benefit in the acute phase. As a further advantage of this experimental paradigm, the authors derive these cells from autologous bone marrow, avoiding the need for potentially confounding immunosuppression.

Few studies have explored the role of endothelial precursor cells in cerebral ischemia/reperfusion, and this is the first to investigate the neuroprotective effects in the acute phase of such therapy. It is likely that the protection offered by these cells derives from additional protective mechanisms (such as the production of growth factors) that merit further investigation. These effects, as well as the potential of these cells to induce neovascularization, provide the opportunity for neurorestoration at later time points than examined in this article (1). Significantly less cumbersome efforts to attenuate endothelial dysfunction in the acute phase of stroke have been previously investigated (adhesion molecule blockade) and have been shown to ultimately fail in the clinical arena.

E. Sander Connolly, Jr.
Andrew F. Ducruet
Ricardo J. Komotar
New York, New York

1. Zhang ZG, Zhang L, Jiang Q, Chopp M: Bone marrow-derived endothelial progenitor cells participate in cerebral neovascularization after focal cerebral ischemia in the adult mouse. **Circ Res** 90:284–288, 2002.

The authors tested the effects of bone marrow-derived EPCs on a rat stroke model. When given immediately after vessel occlusion, behavioral deficits and infarct volumes were reduced. They theorize that these effects were through reduction in endothelial dysfunction, perhaps mediated through nitric oxide. It was interesting to note that the majority of cells were found in the infarct region rather than in other brain locations, a finding noted by others after cell delivery via vascular injection. There are numerous limitations in a study such as this, and these are appropriately addressed in the report. The work is novel and should be pursued further.

Cell delivery two hours after vessel occlusion had reduced effects. Obviously, the temporal nature of any effects needs to be clarified. In the clinical setting, a window of several hours would be imperative. It is interesting to note how few patients actually receive TPA for their stroke, given the time limits on its utility.

Much of the prior work on cellular repair after rodent cerebral infarction has focused on neuronal implantation or striatal tissue grafts. Through an evaluation of endothelial cell effects, this group has chosen a different path that may prove to be an important new avenue for research. Given the number of studies showing measurable behavioral improvement using cellular repair concepts, neurosurgeons should be excited about the future of both basic and clinical research in this area.

Douglas S. Kondziolka
Pittsburgh, Pennsylvania

In this article, the authors present experimental evidence that the intra-arterial administration of autologous ex vivo-expanded bone marrow-derived EPCs is beneficial after focal cerebral ischemia in a rat model. They demonstrate that application of this treatment strategy reduces the volume of infarct and neurological deficits as determined by standard testing in the experimental animals compared with controls after transient occlusion of the middle cerebral artery. In addition, the number of inflammatory cells in the ischemic lesion was also reduced in the treatment group at 24 hours, along with an increase in regional cortical blood flow at 48 hours. As the authors point out, while the beneficial effects of EPC administration may be due, in part, to the attenuation of endothelial dysfunction, other previously identified effects of cellular transplantation may also contribute to the beneficial effect. The use of autologous EPCs is interesting in that it may obviate the need for immunosuppression. It is disappointing that the group receiving the delayed treatment 2 hours after reperfusion did not benefit as much, with obvious implications for ultimate clinical relevance. In addition, the strategy of autologous transplantation requires a prolonged delay between graft harvest, preparation, and transplantation, making it perhaps more appropriate for chronic degenerative disorders than acute ischemia. Nevertheless, the results presented here are interesting and identify endothelial dysfunction as a therapeutic target for treatment of transient focal brain ischemia.

Charles Y. Liu
Los Angeles, California

Ohta et al. characterized EPCs from rat bone marrow for intra-arterial administration after stroke. Behavioral changes were noted and rats were sacrificed for assessment of infarct volume in treated and control groups. Modest improvement in Rota rod (Muromachi, Tokyo, Japan) performance was noted in early-treated rats and a diminution of infarct size was observed. However, there was no statistical difference in mortality in the two groups. They demonstrate the luminal location of injected EPCs and speculate on the mechanism of neuroprotection.

A few additions to the study may help address the feasibility of such cell therapy as a viable treatment option. A less direct method of administration could be tried as opposed to carotid injection. Administration of EPCs could be delayed to better simulate timing of administered therapies, and the period of observation after treatment should be extended to enhance the understanding of the longer-term effects on performance scores and mortality. Additionally, it may be interesting to address the effect of EPC administration on the extent of edema after cerebral ischemia in this model, hypothesizing that improving vascular integrity by limiting endothelial cell dysfunction may reduce cerebral edema, which so often complicates the treatment of patients with large infarcts.

To our knowledge, this is the first report of transplanted bone marrow-derived endothelial cell precursors used as a novel treatment attempt after stroke, and the authors are commended for adding to our existing knowledge of the potential for restorative cell therapy after central nervous system injury. An additional requisite next step is an enhanced understanding into the mechanism of action of transplanted EPCs in this model.

Robert M. Friedlander
Ian F. Dunn
Boston, Massachusetts

Ken-ichiro Kikuta, M.D., Ph.D.
Department of Neurosurgery,
Kyoto University
Graduate School of Medicine,
Kyoto, Japan

Yasushi Takagi, M.D., Ph.D.
Department of Neurosurgery,
Kyoto University
Graduate School of Medicine,
Kyoto, Japan

Yasutaka Fushimi, M.D.
Department of Diagnostic Imaging
and Nuclear Medicine,
Kyoto University
School of Medicine,
Kyoto, Japan

Kouichi Ishizu, M.D., Ph.D.
Department of Diagnostic Imaging
and Nuclear Medicine,
Kyoto University
School of Medicine,
Kyoto, Japan

Tsutomu Okada, M.D.
Department of Diagnostic Imaging
and Nuclear Medicine,
Kyoto University
Graduate School of Medicine,
Kyoto, Japan

Takashi Hanakawa, M.D., Ph.D.
Human Brain Research Center,
Kyoto University
School of Medicine,
Kyoto, Japan

Yukio Miki, M.D., Ph.D.
Department of Diagnostic Imaging
and Nuclear Medicine,
Kyoto University
School of Medicine,
Kyoto, Japan

Hidenao Fukuyama, M.D., Ph.D.
Human Brain Research Center,
Kyoto University
School of Medicine,
Kyoto, Japan

Kazuhiko Nozaki, M.D., Ph.D.
Department of Neurosurgery,
Kyoto University
Graduate School of Medicine,
Kyoto, Japan

Nobuo Hashimoto, M.D., Ph.D.
Department of Neurosurgery,
Kyoto University
Graduate School of Medicine,
Kyoto, Japan

Reprint requests:
Ken-ichiro Kikuta, M.D., Ph.D.,
Department of Neurosurgery,
Kyoto University
Graduate School of Medicine,
54 Kawaharacho,
Shogoin, Sakyo-ku,
Kyoto 606-8507, Japan.
Email: kikuta@kuhp.kyoto-u.ac.jp

Received, December 28, 2005.
Accepted, June 1, 2006

"Target Bypass": A Method for Preoperative Targeting of a Recipient Artery in Superficial Temporal Artery-to-Middle Cerebral Artery Anastomoses

OBJECTIVE: To introduce a method for preoperative targeting of a proper recipient artery in superficial temporal artery-to-middle cerebral artery anastomosis.

METHODS: Six operations for superficial temporal artery-to-middle cerebral artery anastomosis in four patients with moyamoya disease or moyamoya-like disease and two operations in two patients with atherosclerotic cerebrovascular occlusive disease accompanied by coronary artery stenosis were performed using our method. Before surgery, a 3-Tesla magnetic resonance imaging study was performed with axial T1-weighted three-dimensional magnetization-prepared rapid acquisition gradient-echo sequences and three-dimensional time-of-flight magnetic resonance angiography. Data on quantitative regional cerebral blood flow were obtained by iodine-123-labeled N-isopropyl-iodoamphetamine single-photon emission computed tomography or positron emission computed tomography. The magnetic resonance angiography and regional cerebral blood flow data sets were registered with the magnetization-prepared rapid acquisition gradient-echo data set by means of the coregistration function of the SPM2 software. We examined the arteries located on or near the cortex where the regional cerebral blood flow had significantly decreased and used the coregistered data set and MRIcro software to select the cortical artery with the largest diameter as the target recipient artery. At the surgery, the data sets were applied to the neuronavigation system and the actual site of the target was confirmed in the operation before scalp incision. The superficial temporal artery was anastomosed with the target through a small craniotomy.

RESULTS: Successful bypass surgery to the target was confirmed in all cases.

CONCLUSION: The "target bypass" method might be effective for cases with moyamoya disease or for cases requiring surgery through a small craniotomy.

KEY WORDS: Cerebral blood flow, Coregistration, Moyamoya disease, Neuronavigation, Recipient, Superficial temporal artery-to-middle cerebral artery anastomosis, Target

Neurosurgery 59[ONS Suppl 4]:ONS-320–ONS-327, 2006 DOI: 10.1227/01.NEU.0000232775.06672.F4

Superficial temporal artery-to-middle cerebral artery (STA-MCA) anastomosis was first reported by Yaşargil (22) in 1969. In Japan, STA-MCA has especially been applied to the treatment of moyamoya disease (MMD) (8, 13), a progressive steno-occlusive disease at the terminal portion of the bilateral internal carotid arteries (ICAs) with the development of moyamoya vessels as collateral channels (4). Although direct bypass is reported to be more effective than indirect bypass, such as encephaloduroarteriosynangiosis, for improved clinical and radiological treatment of MMD (2, 7, 10, 12, 18), it is often disregarded because of its technical difficulty (11). One reason is the difficulty of finding suitable recipient arteries during the operation because the diameter of most cortical branches of the MCA is small in patients with MMD (9, 10, 13). Recent advances in neuroradiology

TABLE 1. Patient characteristics[a]

Patient no.	Age (yr)/sex	Disease entity	Side	Procedure	Diameter of craniotomy (mm)
1	29/M	MMD	Left	STA-MCA	25
			Right	STA-MCA	20
2	67/F	MMD	Right	STA-MCA + EMS	40
3	57/F	Moyamoya-like disease underlying diabetes mellitus	Right	STA-MCA	30
			Left	STA-MCA	20
4	63/F	MMD	Left	STA-MCA	20
5	73/M	ICA occlusion accompanied with coronary artery stenosis	Left	STA-MCA	20
6	71/M	MCA occlusion accompanied with coronary artery stenosis	Right	STA-MCA	20

[a] MMD, moyamoya disease; STA-MCA, superficial temporal artery-to-middle cerebral artery; EMS, encephalo-myo-synangiosis; ICA, internal carotid artery.

and image-guided navigation surgery have resulted in the surgical use of fusion images obtained through various kinds of neuroradiological studies (1, 6, 17). Here, we present a method for the preoperative targeting of an appropriate recipient artery in STA-MCA anastomosis and introduce our initial experiences applying our method for cerebrovascular occlusive disease, such as MMD.

Patient Summary

Six operations for STA-MCA anastomosis in four patients with MMD or moyamoya-like disease and two operations in two patients with atherosclerotic cerebrovascular occlusive disease accompanied with coronary artery stenosis were performed using our method. *Table 1* shows the characteristics of the patients.

Imaging Study and Data Processing

Before surgery, a magnetic resonance imaging study was performed with a 3-Tesla magnetic resonance scanner (Magnetom Trio; Siemens, Erlargen, Germany) with magnetization-prepared rapid acquisition gradient-echo (MPRAGE) sequences (repetition time [TR], 2000; echo time [TE], 4.4; time interval [TI], 990 ms; flip

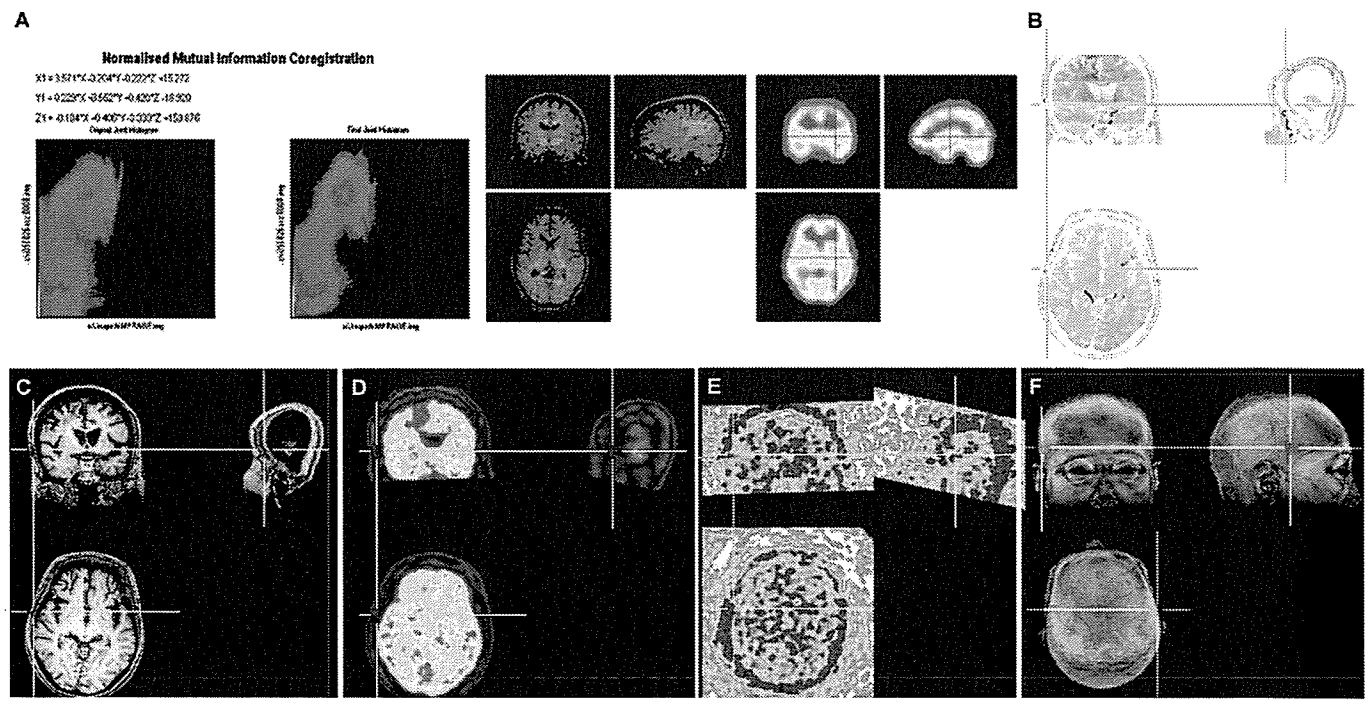

FIGURE 1. A, *MRA and rCBF data sets were registered with the MPRAGE data set by means of the coregistration function of the SPM2 software to render the registered data set available with the anatomic information of MPRAGE. By using MRIcro software and adjusting the slice and the region of interest* (cross bar), *we obtained coregistered three-dimensional images showing the arteries of the head* (B), *the anatomic structures of the brain* (C), *the distribution of the rCBF* (D), *the distribution of the regional oxygen extraction fraction* (E) *(only in cases with PET studies), and the surface of the scalp* (F).

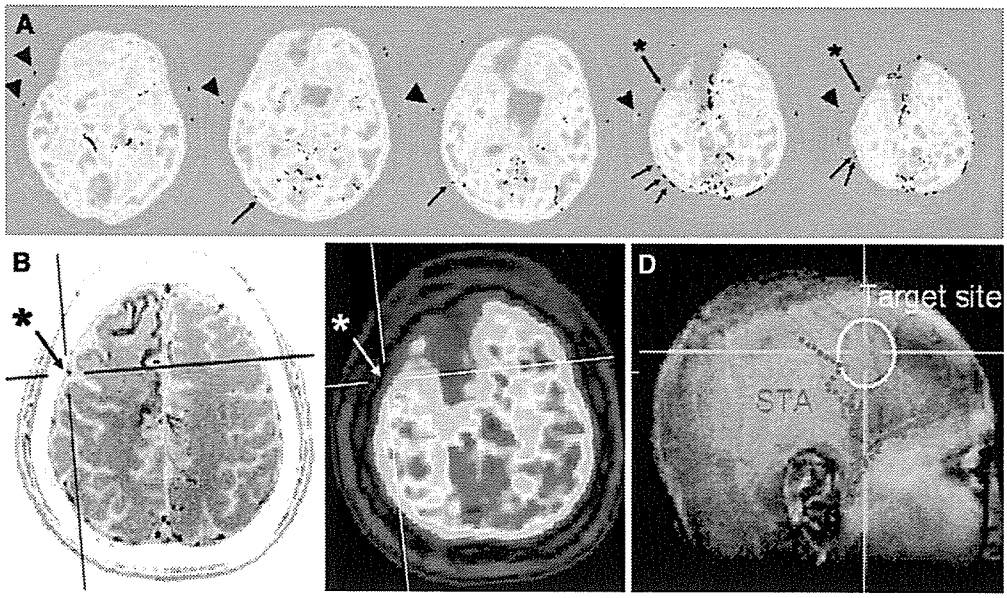

FIGURE 2. A–C, *fusion images between the MRA and rCBF data sets were obtained using the MRIcro software. Candidate recipient arteries could be found on the cortex of the right hemisphere* (arrowheads, *STA;* arrows, *candidate recipient arteries). As for the target* (asterisks *in* A–C), *we selected the cortical artery with the largest diameter from the candidates located on or near the cortex where the rCBF was markedly decreased.* D, *the location of the target in the coregistered scalp images was visible, which provided the site of the craniotomy.*

angle, 8 degrees; matrix, 256 × 240; field of view, 24 cm; 208 slices; slice thickness, 1 mm; no interslice gap; single averaging) and three-dimensional time-of-flight magnetic resonance angiography (MRA) (TR, 22 ms; TE, 3.84 ms; flip angle, 18 degrees; slice thickness, 0.64 mm; matrix, 512 × 208; acquisition time, 5 min 24 s; 192 slices) (5, 16). Quantitative regional cerebral blood flow (rCBF) was evaluated by iodine-123-labeled N-isopropyl-iodoamphetamine-single-photon emission computed tomography with a three-head rotating gamma camera (PRISM 3000; Shimazu Co., Ltd., Kyoto, Japan) or a $^{15}O_2$ gas steady-state positron emission computed tomography (PET) study with a PET scanner (Advance; General Electric, Milwaukee, WI) as reported previously (15, 19, 21). The MRA and rCBF data sets were registered with the MPRAGE data set through the coregistration function of the SPM2 software (Wellcome Department of Imaging Neuroscience, London, England) to create a registered data set with anatomic information of MPRAGE (*Fig. 1A*). Postoperative 3-Tesla magnetic resonance and single-photon emission computed tomographic studies were performed between 2 weeks and 1 month after the surgeries.

Preoperative Targeting of the Recipient Artery

By adjusting the slice and the region of interest with free MRIcro software (http://www.mricro.com/) and using the coregistered data set of MPRAGE, MRA, and rCBF, it is possible to obtain coregistered three-dimensional images showing the arteries in the head (*Fig. 1B*), the anatomic structures of the brain (*Fig. 1C*), the distribution of the rCBF (*Fig. 1D*), the distribution of the regional oxygen extraction fraction (*Fig. 1E*) (only in cases with PET studies), and the surface of the scalp (*Fig. 1F*) (18). This software also enables the fusion of MRA and rCBF images (*Fig. 2A*). Some candidate arteries for the surgery can be found in these consecutive fusion images (*Fig. 2A*). From them, we selected as the target the artery with the largest diameter that was located on or near the cortex where rCBF was markedly decreased (*Fig. 2, B* and *C*). The location of the target in the coregistered scalp images could also be detected, which provided the site for the craniotomy (*Fig. 2D*). This approach enabled preoperative targeting of a recipient artery.

Operative Procedures

On the day before surgery, a three-dimensional high-resolution computed tomographic scan of the whole brain was obtained with a 64-detector-row computed tomographic scanner (Aquilion; Toshiba Medical, Tokyo, Japan) to obtain the reference images. The rCBF, MRA, and three-dimensional computed tomographic data sets were applied to the neuronavigation system (Stealth Station; Medtronic, Sofamor Danek, Memphis, TN) and the fusion process was carried out with these images (6). With the patient under general anesthesia, we made the scalp incision after determining the location of the target on the scalp (*Fig. 3A*). The actual location of the target beneath the scalp was revealed through the navigation system, which displayed images of the cranium (*Fig. 3B*), MRA (*Fig. 3C*), and rCBF imaging (*Fig. 3D*), as well as a magnified image of the MRA (*Fig. 3E*). The location of the craniotomy and the design of the scalp incision were determined according to the location of the target and course of the STA (*Fig. 3, F* and *G*). After performing a small craniotomy (*Fig.3H*) and dural incision, we exposed the target at the center of the craniotomy (*Fig. 3I*). The STA was successfully anastomosed to the target (*Fig. 3J*).

RESULTS

All surgeries were performed through a relatively small craniotomy. The patency of the bypass to the target and the postoperative improvement of rCBF was confirmed in all cases by coregistered images between MRA and rCBF imaging (*Table 1*).

ILLUSTRATIVE CASES

Patient 3

A 56-year-old woman with moyamoya-like disease underlying diabetes mellitus was admitted to our institution after a second cerebral

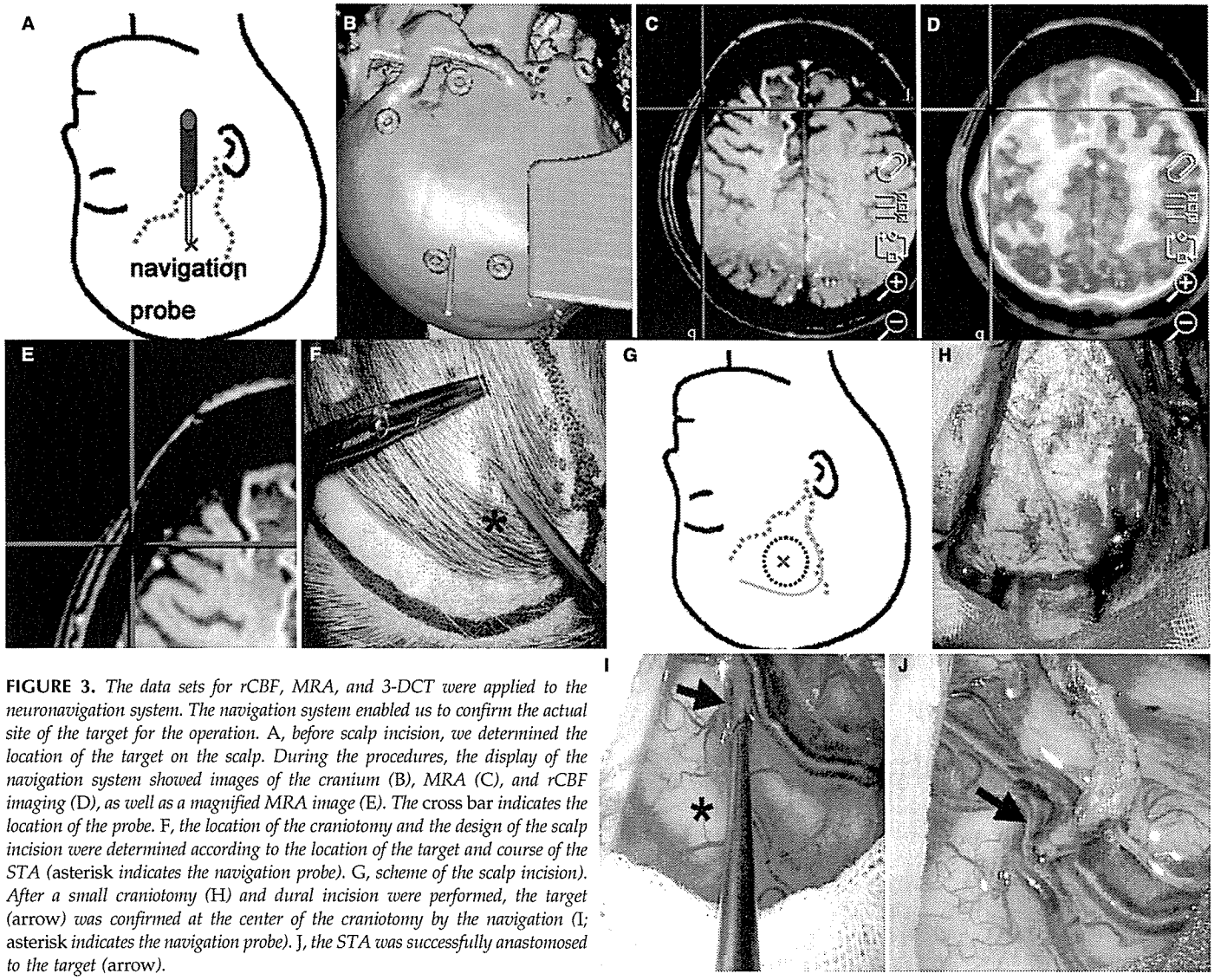

FIGURE 3. *The data sets for rCBF, MRA, and 3-DCT were applied to the neuronavigation system. The navigation system enabled us to confirm the actual site of the target for the operation.* A, *before scalp incision, we determined the location of the target on the scalp. During the procedures, the display of the navigation system showed images of the cranium* (B), *MRA* (C), *and rCBF imaging* (D), *as well as a magnified MRA image* (E). *The* cross bar *indicates the location of the probe.* F, *the location of the craniotomy and the design of the scalp incision were determined according to the location of the target and course of the STA* (asterisk *indicates the navigation probe).* G, *scheme of the scalp incision). After a small craniotomy* (H) *and dural incision were performed, the target* (arrow) *was confirmed at the center of the craniotomy by the navigation* (I; asterisk *indicates the navigation probe).* J, *the STA was successfully anastomosed to the target* (arrow).

infarction in the right frontal lobe (*Fig. 4A*). Before surgery, she presented with transient ischemic attacks of the left hemiparesis occurring several times a day. A preoperative single-photon emission computed tomographic study revealed a significant decrease in rCBF (*Fig. 4B*) and regional cerebrovascular reserve under acetazolamide challenging dominantly in the right frontal lobe. Cerebral angiography revealed a right MCA occlusion (*Fig. 4, C and D*) and stenosis at the terminal portion of the left ICA (*Fig. 4, E and F*). STA-MCA anastomosis on the right side was planned. Although few cortical branches of the right MCA could be visualized in the angiograms, our method enabled preoperative targeting of a recipient artery in the right frontal lobe (*Figs. 2 and 3*). Postoperative studies revealed the patency of the bypass to the target (*Fig. 4, G and H*) through improved rCBF in the right hemisphere (*Fig. 4I*). This patient's transient ischemic attacks disappeared after surgery.

Patient 4

A 63-year-old woman with MMD presented with incomplete Gerstmann's syndrome caused by completed stroke. She underwent left STA-MCA anastomosis. Preoperative targeting of a recipient artery (*Fig. 5, A–C*) and bypass surgery were performed in the same manner as in Patient 3. We exposed the targeted recipient artery at the center of the craniotomy (*Fig. 5, E and F*) through a quarter-sized craniotomy. The STA was successfully anastomosed to the target (*Fig. 5G*).

DISCUSSION

STA-MCA anastomosis was first reported by Yaşargil (22) in 1969. Although the international trial in 1985 (3) failed to prove this surgery's prophylactic effects against recurrent stroke (3), the Japanese extracranial-intracranial bypass trial (JET study) completed its evaluation of the validity of STA-MCA anastomosis in intracranial arterial occlusive disease in preventing hemodynamic stroke (15). Moreover, a carotid occlusion surgery study is ongoing in the United States.

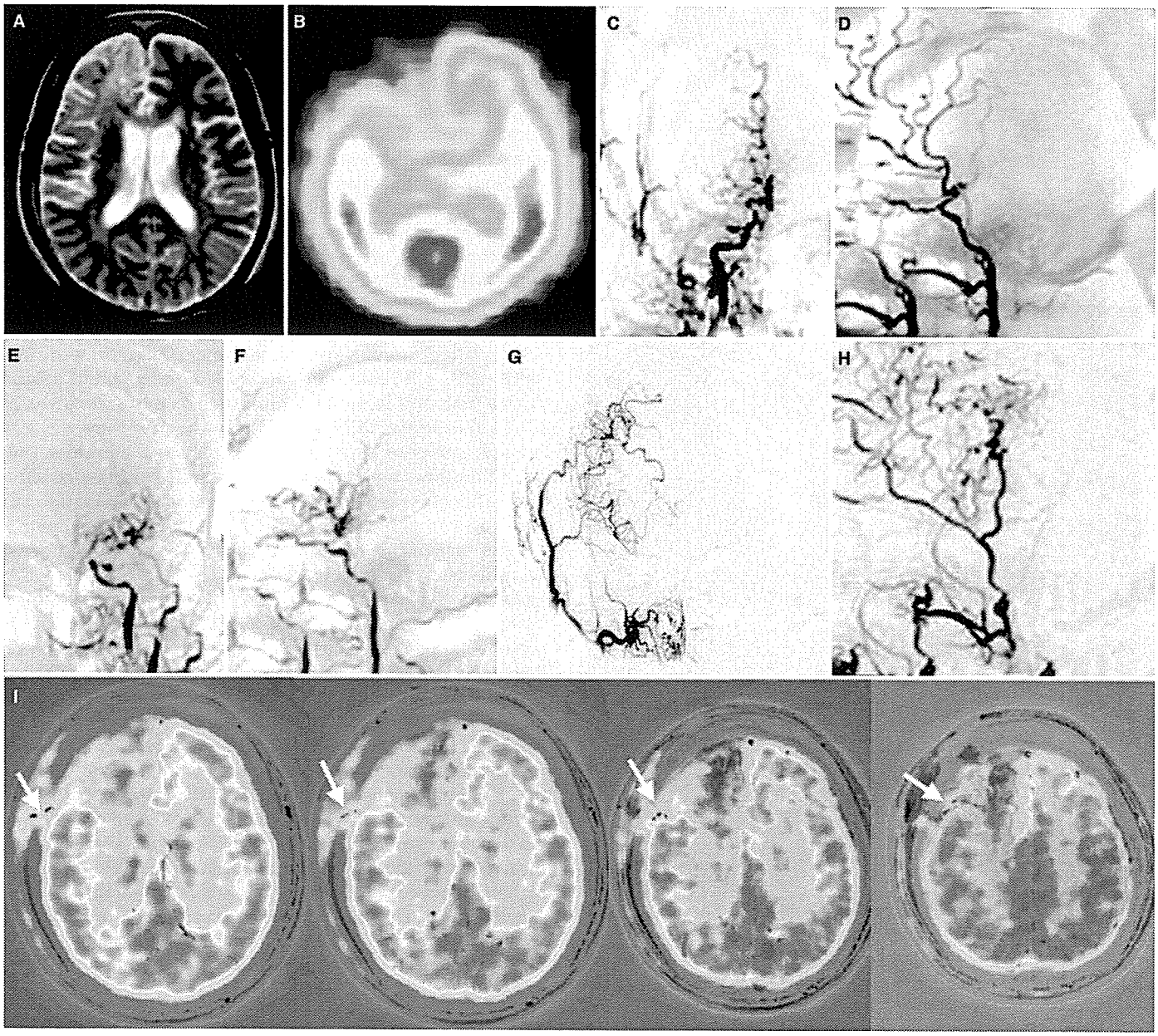

FIGURE 4. *Right STA-MCA anastomosis for a 56-year-old woman (Patient 3) with moyamoya-like disease.* A, *T2-weighted magnetic resonance imaging scan obtained on admission demonstrating cerebral infarction in the right frontal lobe.* B, *a preoperative single-photon emission computed tomographic study revealing significantly decreased rCBF, mainly in the right frontal lobe.* C–F, *cerebral angiography revealing right MCA* (C *and* D) *occlusion and stenosis at the terminal portion of the left ICA* (E *and* F). *Postoperative external angiograms in the anteroposterior* (G) *and lateral* (H) *views showing the patency of the bypass.* I, *postoperative fusion images between the MRA and rCBF showed the success of the bypass to the target* (arrows) *with improvement in rCBF in the right hemisphere.*

In Japan, STA-MCA anastomosis has especially been applied to the treatment of MMD (8, 13). Although direct bypass surgery, such as STA-MCA anastomosis, was reported to be more effective than indirect anastomosis in the treatment of MMD (2, 7, 10, 12, 18), indirect bypass methods, such as encephaloduroarteriosynangiosis, have often been preferred because of the technical difficulty of direct bypass (12). Moreover, in addition to the technical difficulty of the anastomotic procedure itself, finding recipient arteries with a suitable diameter for anastomosis is difficult during surgery for MMD (8, 9, 12). In our institution, STA-MCA anastomosis has been performed in all cases of MMD or moyamoya-like disease (13). Although the results of our surgery have been quite favorable, a relatively large craniotomy in the frontotemporal region is

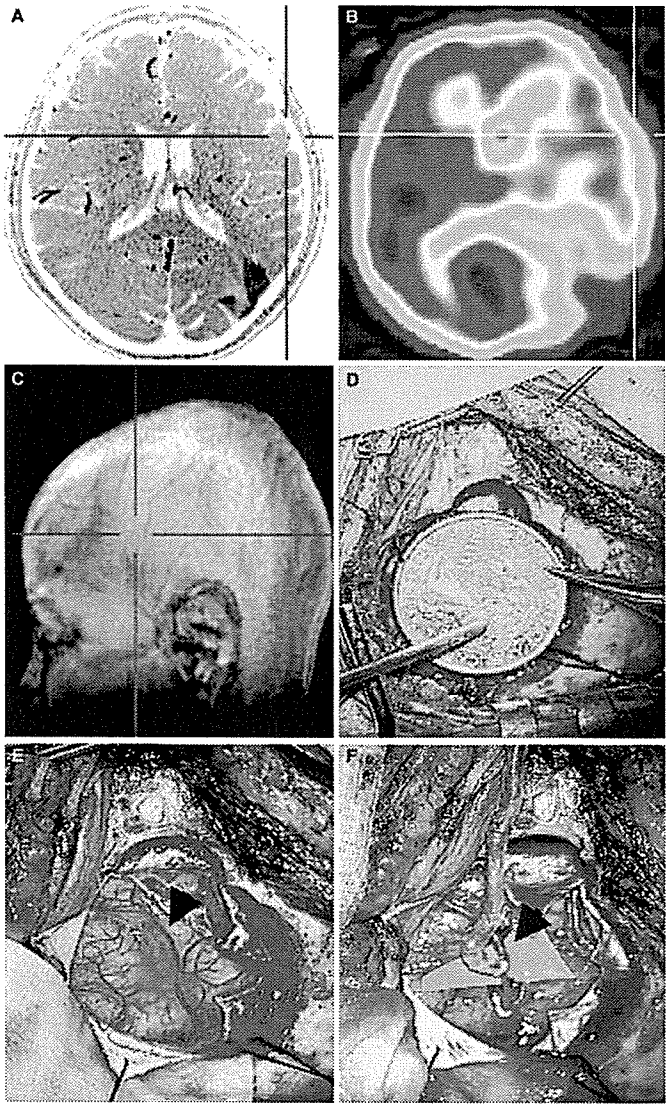

FIGURE 5. *Left STA-MCA anastomosis in a 63-year-old woman with MMD (Patient 4). Preoperative targeting of a recipient artery* (A, *MRA;* B, *rCBF;* C, *scalp imaging) and bypass surgery in the same manner as in Patient 3. A craniotomy the size of a quarter* (D) *was used to expose the targeted recipient artery at the center of the craniotomy* (E) *and enabled success bypass to the target* (F). *Target indicated by* arrowheads.

routinely required to reveal a proper recipient artery for the operation (8, 13).

One of the advantages of our method is the identification of the location of the recipient artery with pinpoint accuracy before scalp incision. Even in cases, such as those of MMD, in which preoperative angiograms demonstrate only a few candidates for recipient artery, an appropriate recipient artery can be exposed at the center of craniotomy with our method. Therefore, our method is considered effective in surgery for most cases of MMD.

A second advantage of our method is the use of a small craniotomy for STA-MCA anastomosis. In this study, bypass surgery could be performed through a small craniotomy, even in patients with MMD. However, in some MMD patients, especially pediatric patients, an indirect bypass, such as encephalomyo-synangiosis, should be combined with a direct bypass through a large craniotomy (13). Thus, we do not recommend surgery through a small craniotomy with our method for all cases of MMD. Bypass surgery through a small craniotomy is also indicated for cases in which surgery must be performed quickly. Our method might be useful in STA-MCA anastomotis for patients with systemic disease, such as a heart dysfunction.

In this study, we performed three-dimensional time-of-flight MRA with a 3-Tesla unit to target a recipient artery. MRA principally describes only arteries because it selectively detects and captures signals moving at high velocity. As reported previously, three-dimensional time-of-flight MRA with a 3-Tesla unit can well describe small arteries with a diameter less than 1 mm, such as moyamoya vessels (5). In this study, MRA also clearly described arteries having a diameter of approximately 1 mm on the brain surface or within the scalp. Although brain shift has been raised as a significant issue with image-guided neuronavigation surgery (6), it was not a significant problem with our method because use of the navigation system was concluded before scalp incision.

A third advantage of our method is the targeting of a recipient artery with reference to an rCBF map to achieve selective revascularization of the region with decreased rCBF. In this report, among the arteries situated on or near the cortex where rCBF was significantly decreased, we selected the cortical artery with the largest diameter as the target. However, whether or not our approach for determining the target is the best for preventing recurrent stroke remains controversial, and this might be one of the greatest problems with our method. It is possible that the best target is an artery with the largest diameter located other than in the region presenting decreased rCBF. An artery in the cortex in the region with the most significant decrease in rCVR (23) or with highest increase in rOEF in the PET study (20) might be a more suitable target. This issue should be investigated further.

CONCLUSION

The "target bypass" method can provide preoperative identification of the location of a proper recipient artery in STA-MCA anastomosis. This method might be effective for patients with MMD or those requiring surgery through a small craniotomy. Methods of determining the optimal target recipient artery should be further investigated.

REFERENCES

1. Coenen VA, Krings T, Weidemann J, Hans FJ, Reinacher P, Gilsbach JM, Rohde V: Sequential visualization of brain and fiber tract deformation during intracranial surgery with three-dimensional ultrasound: An approach to evaluate the effect of brain shift. **Neurosurgery** 56 [Suppl 1]:133–141, 2005.
2. Cahan LD: Failure of encephalo-duro-arterio-synangiosis procedure in moyamoya disease. **Pediatr Neurosci** 12:58–62, 1985.

3. EC/IC Bypass Study Group: Failure of extracranial-intracranial arterial bypass to reduce the risk of ischemic stroke. Results of an international randomized trial. **N Engl J Med** 313:1191–1200, 1985.
4. Fukui M: Guidelines of the diagnosis and treatment of spontaneous occlusion of the circle of Willis (moyamoya disease). **Clin Neurol Neurosurg** 99 [Suppl 2]:S238–S240, 1997.
5. Fushimi Y, Miki Y, Kikuta K, Kanagaki M, Yamamoto A, Nozaki K, Hashimoto N, Hanakawa T, Fukuyama H, Togashi K: Comparison of 3.0- and 1.5-T three-dimensional time-of-flight MR angiography in moyamoya disease: A preliminary study. **Radiology** 239:232–237, 2006.
6. Gralla J, Guzman R, Brekenfeld C, Remonda L, Kiefer C: High-resolution three-dimensional T2-weighted sequence for neuronavigation: A new setup and clinical trial. **J Neurosurg** 102:658–663, 2005.
7. Houkin K, Kuroda S, Ishikawa T, Abe H: Neovascularization (angiogenesis) after revascularization in moyamoya disease. Which technique is most useful for moyamoya disease? **Acta Neurochir (Wien)** 142:269–276, 2000.
8. Karasawa J, Kikuchi H, Furuse S, Kawamura J, Sakaki T: Treatment of moyamoya disease with STA-MCA anastomosis. **J Neurosurg** 49:679–688, 1978.
9. Kawashima M, Rhoton AL Jr, Tanriover N, Ulm AJ, Yasuda A, Fujii K: Microsurgical anatomy of cerebral revascularization. Part I: Anterior circulation. **J Neurosurg** 102:116–131, 2005.
10. Matsushima T, Inoue T, Suzuki SO, Fujii K, Fukui M, Hasuo K: Surgical treatment of moyamoya disease in pediatric patients—Comparison between the results of indirect and direct revascularization procedures. **Neurosurgery** 31:401–405, 1992.
11. Matsushima Y, Inaba Y: Moyamoya disease in children and its surgical treatment. Introduction of a new surgical procedure and its follow-up angiograms. **Childs Brain** 11:155–170, 1984.
12. Miyamoto S, Kikuchi H, Karasawa J, Nagata I, Yamazoe N, Akiyama Y: Pitfalls in the surgical treatment of moyamoya disease. Operative techniques for refractory cases. **J Neurosurg** 68:537–543, 1988.
13. Miyamoto S, Nagata I, Hashimoto N, Kikuchi H: Direct anastomotic bypass for cerebrovascular moyamoya disease. **Neurol Med Chir (Tokyo)** 8 [Suppl]:294–296, 1998.
14. Mizumura S, Nakagawara J, Takahashi M, Kumita S, Cho K, Nakajo H, Toba M, Kumazaki T: Three-dimensional display in staging hemodynamic brain ischemia for JET study: Objective evaluation using SEE analysis and 3D-SSP display. **Ann Nucl Med** 18:13–21, 2004.
15. Nishizawa S, Yonekura Y, Tanaka F, Fujita T, Tsuchimochi S, Ishizu K, Okazawa H, Tamaki N, Konishi J: Evaluation of a double-injection method for sequential measurement of cerebral blood flow with iodine-123-iodoamphetamine. **J Nucl Med** 36:1339–1345, 1995.
16. Okada T, Mikuni N, Miki Y, Kikuta K, Urayama S, Hanakawa T, Fushimi Y, Yamamoto A, Kanagaki M, Fukuyama H, Hashimoto N, Togashi K: Integration of diffusion tensor tractography of the corticospinal tract using 3T with intraoperative white matter stimulation mapping: Preliminary result to validate corticospinal tract localization. **Radiology** (in press).
17. Roden C, Brett M: Stereotaxic display of brain lesions. **Behav Neurol** 12: 191–200, 2000.
18. Touho H, Karasawa J, Ohnishi H, Yamada K, Shibamoto K: Surgical reconstruction of failed indirect anastomosis in childhood moyamoya disease. **Neurosurgery** 32:935–940, 1993.
19. Ueno M, Nishizawa S, Toyoda H, Shimono T, Miyamoto S, Hashimoto N, Konishi J: Assessment of cerebral hemodynamics before and after revascularization in patients with occlusive cerebrovascular disease by means of quantitative IMP-SPECT with double-injection protocol. **Ann Nucl Med** 15:209–15, 2001.
20. Yamauchi H, Fukuyama H, Nagahama Y: Significance of increased oxygen extraction fraction in five-year prognosis of major cerebral arterial occlusive disease. **J Nucl Med** 40:1992–1998, 1999.
21. Yamauchi H, Fukuyama H, Nagahama Y, Nishizawa S, Konishi J: Uncoupling of oxygen and glucose metabolism in patients with crossed cerebella diaschisis. **Stroke** 30:1424–1428, 1999.
22. Yaşargil MG: Anastomosis between the superficial temporal artery and a branch of the middle cerebral artery, in Yaşargil MG (ed): *Microsurgery Applied to Neurosurgery*. Stuttgart, George Thieme Verlag, 1969, pp 105–115.
23. Yokota C, Hasegawa Y, Minematsu K: Effect of acetazolamide reactivity on long-term outcome in patients with major cerebral artery occlusive diseases. **Stroke** 29:640–644, 1998.

COMMENTS

In this article, the authors have described the preoperative targeting of the superficial temporal artery-to-middle cerebral artery (STA-MCA) bypass using preoperative study of cerebral blood flow and fusion of this information with other imaging data. They used it successfully in patients with moyamoya syndrome. This seems to be a good strategy in the short term. Over the long term, however, the bypass donor artery is expected to enlarge and supply a much larger vascular territory through collateral circulation, and the technique may be less important.

An important issue to be considered is that the ischemic territory of the brain undergoes additional ischemia during the bypass procedure, and may be more susceptible to a stroke. The question would be whether or not it is better to place the bypass in the penumbra zone of the ischemic territory because, in time, the donor vessel would be expected to also supply the densely ischemic region.

In the United States, vascular bypasses for ischemia (not aneurysms or basal tumors) are routinely performed only for moyamoya syndrome. For patients with atherosclerotic occlusive disease, such bypasses are being reimbursed by Medicare only as part of the Carotid Occlusion Surgery Study trial, even though there are patients who have failed maximal medical therapy and, for one reason or another, do not qualify for the Carotid Occlusion Surgery Study trial. This is not true in Japan, where STA-MCA bypasses are still being performed in large numbers for cerebral ischemia secondary to atherosclerotic vascular occlusion.

Laligam N. Sekhar
Seattle, Washington

Kikuta et al. apply multiple imaging modalities (magnetic resonance angiography [MRA] and three-dimensional [3-D] computed tomographic scanning) to target the donor STA and an appropriate sized MCA recipient branch in moyamoya disease or moyamoya-like disease. In addition, the authors use various cerebral blood flow studies (single-photon emission computed tomography and positron emission tomography [PET]) to determine regions of hypoperfusion for targeting in these patients. This technique was successful in six (STA-MCA) bypass operations. The authors admit that this is a technical report and do not provide evidence that this will help patient outcome. However, this article is important because it may reduce the number of indirect bypass procedures that are used because of inadequate recipient arteries, and it allows for a smaller craniotomy, which may reduce operative time and, possibly, morbidity. The authors appropriately state that it remains unclear whether or not targeting a recipient artery in areas of hypoperfusion is beneficial to patient outcome. One limitation of this study is that it only involves six study subjects. However, the technique is extremely novel and seems feasible. Further experience with this method, combined with assessment of clinical outcomes, will determine its efficacy.

Gary K. Steinberg
Michael E.B. Kelly
Stanford, California

The authors have developed a technique using a unique software application by which a revascularization procedure can be targeted very specifically to a certain area of cerebral cortex that appears maxi-

mally threatened on physiological imaging. To accomplish this, 3 T magnetic resonance imaging scans, magnetization prepared rapid gradient echo-water excitation, 3-D time-of-flight, MRA, and color Doppler flow studies with either single-photon emission computed tomography or PET are acquired preoperatively. At surgery, the color Doppler flow and MRA images are coregistered with the 3-D high-resolution computed tomographic scan to perform intraoperative localization. As a result, very small craniotomies are possible to direct flow from an extracranial to intracranial bypass into a very specific area.

This is an interesting and intuitive application of current image fusion techniques. It enables the surgeon to target a specific recipient artery that is size matched to the donor STA. Potential difficulties in applying this technique include considerations of whether or not the STA maintains adequate diameter once you reach a peripheral target. In addition, one wonders if it might be more appropriate to target a larger recipient (with a larger donor) more proximally along the arterial tree to the area of maximal ischemia. Possibly, in using that mechanism, even more flow could be directed to the specific target region. Nevertheless, this is an interesting study that should stimulate all of us to be more creative as we approach patients with complicated ischemic state.

H. Hunt Batjer
Chicago, Illinois

The authors have described an innovative technique to preoperatively identify the recipient artery when performing STA-MCA anastomosis. Images of the angioarchitecture are obtained by MRA and fused with regional cerebral blood flow examinations obtained either by single-photon emission computed tomography or PET. The authors were able to coregister 3-D images of the arteries, the anatomic structures of the brain, and the distribution of the regional cerebral blood flow or regional oxygen extraction fraction (if PET studies were used). This allowed the authors to identify the recipient artery on the basis of diameter as well as region of decreased cerebral blood flow.

The primary advantages of this technique, as expressed by the authors, include the ability to use a very small craniotomy by preselecting the recipient artery and the ability to identify the region of decreased cerebral blood flow. Although the size of the craniotomy for an extracranial to intracranial bypass does not dictate the length of the operation to any great degree, there is some benefit of being able to preoperatively identify a recipient artery of adequate size. Whether or not a bypass performed in an area of greater decreased cerebral blood flow is advantageous remains to be proven. Patients with moyamoya disease or MCA occlusion may well redistribute the additional blood flow through the patent anastomosis to the regions of ischemia. Certainly, further work is indicated to determine the precise benefit of this technique. Notwithstanding these cautionary comments, the authors have demonstrated an elegant technique for identifying a suitable recipient vessel for extracranial to intracranial bypass in a highly reproducible manner.

Daniel L. Barrow
Atlanta, Georgia

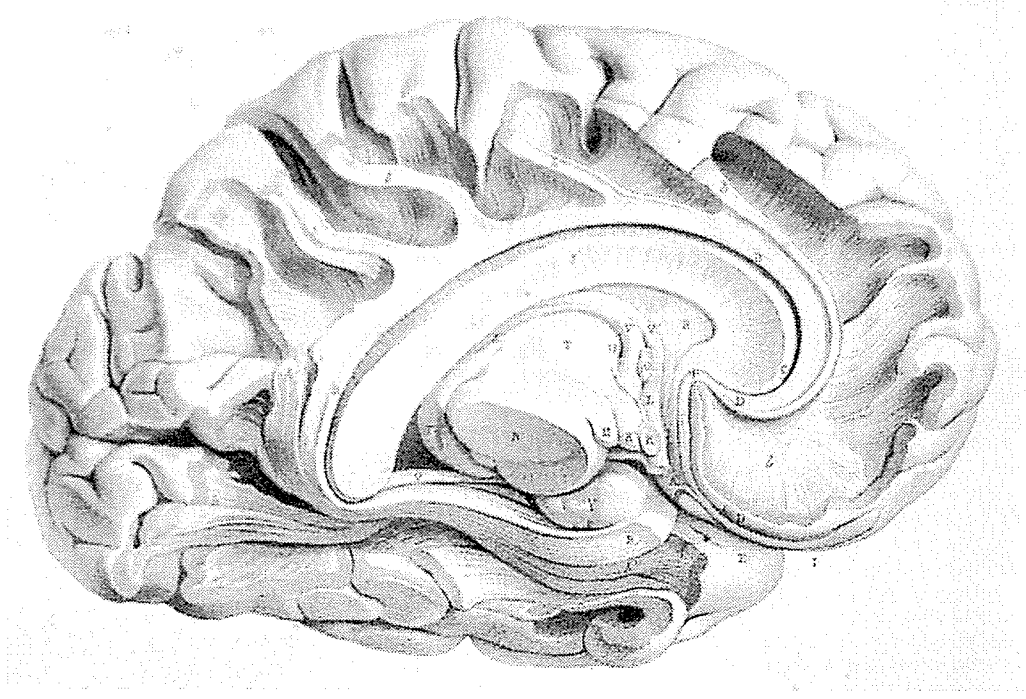

Achille Louis Foville, 1799-1978, ***Traité Complet de l'anatomie, de la Physiologie et de la Pathologie du Système Nerveux Cérébro-spinal.*** *Paris: Fortin, Masson, 1844 (Courtesy, Rare Book Room, Norris Medical Library, Keek School of Medicine, University of Southern California, Los Angeles, California.)*

モヤモヤ病（ウィリス動脈輪閉塞症)調査研究班　名簿

区分	氏名	所属など	職名
主任研究者	橋本信夫	京都大学大学院医学研究科脳病態生理学講座脳神経外科	教授
分担研究者	寶金清博	札幌医科大学医学部脳神経外科学講座	教授
	冨永悌二	東北大学大学院医学系研究科神経外科学神経科学	教授
	宮本享	国立循環器病センター脳神経外科	部長
	鈴木則宏	慶応義塾大学医学部神経内科学	教授
	野川茂	東京歯科大学市川総合病院内科学	助教授
	中川原譲二	中村記念病院脳神経外科	部長
	小泉昭夫	京都大学医学研究科社会医学専攻系環境衛生学分野	教授
	北川一夫	大阪大学大学院循環器内科学医学研究科	講師
	永田泉	長崎大学医歯薬学総合研究科病態解析制御学	教授
	黒田敏	北海道大学大学院医学研究科神経病態学講座脳神経外科	講師
	菊田健一郎	京都大学大学院医学研究科脳病態生理学講座脳神経外科	助手

類もやもや病　診断の手引き

内頚動脈終末部、前および中大脳動脈近位部に狭窄、閉塞を認め、その付近に異常血管網が観察され、脳血管病変をきたしうる基礎疾患を有する場合を、類もやもや病　と診断する。片側性、両側性は問わない。類もやもや病を診断するに当たっては、脳血管狭窄、閉塞をきたすことが容易に想像される疾患（下記Ａ）と脳血管病変への直接的な関与が明らかでない疾患（下記Ｂ）を記載しておくことが望ましい。後者の方が、もやもや病と同様の機序により脳血管病変を来している可能性が高い。類もやもや病と診断された場合、もやもや血管の出現がもやもや病同様に脳血行動態不全を反映している可能性が高く、将来の脳梗塞の発症を予防するため積極的に脳循環動態評価を行い、血行再建術の適応を考慮する必要がある。

基礎疾患の分類

Ａ：脳血管病変の直接的な関与が想定される疾患

動脈硬化、動脈解離、線維筋異形成、放射線照射、脳腫瘍（血管増生因子産生）、髄膜炎、自己免疫疾患・血管炎（ＳＬＥ，結節性多発動脈炎などを含む）、頭部外傷、凝固因子異常（プロテインＣ欠損症、プロテインＳ欠損症、プラスミノーゲン欠損症）

Ｂ：脳血管病変への関与が明らかでないが関連が示唆される疾患

ダウン症候群、レックリングハウゼン病、甲状腺機能亢進症、サラセミア、ターナー症候群、川崎病、腎動脈狭窄、網膜色素沈着症、結節性硬化症、弾性線維性偽黄色腫、鎌状赤血球症、多発性嚢胞腎、咽頭炎、扁桃腺炎、シェーグレン症候群、Ｉ型糖原病(von Gierke 病)、好酸球性肉芽腫症、レプトスピラ症

「ウィリス動脈輪閉塞症における病態・治療に関する研究」
平成 18 年度総括・分担研究報告書
編集　京都大学脳神経外科　菊田健一郎